

# Trishomocyclopropenylum Cations. Structure, Stability, Magnetic Properties, and Rearrangement Possibilities

Kalman J. Szabo, Elfi Kraka, and Dieter Cremer\*

Department of Theoretical Chemistry, University of Göteborg, Kemigården 3, S-412 96 Göteborg, Sweden

Received October 30, 1995<sup>§</sup>

Potentially trishomoaromatic cations possessing the 6-X-bicyclo[3.1.0]hex-3-yl (X = CH<sub>2</sub>, BH, NH, O) or bicyclo[3.2.0]hept-3-yl unit have been investigated at the Hartree–Fock, second-order, third-order, and fourth-order (single, double, quadruple excitations) Møller–Plesset perturbation level employing the 6-31G(d) basis set. IGLO/6-31G(d) chemical shift calculations have been carried out at optimized geometries. Through-space interactions between the symmetric Walsh orbital of the three-membered ring and  $p\pi(C3)$  orbital have been analyzed as a function of orbital energies and orbital overlap. The best indicators for trishomoaromaticity are NMR chemical shifts and magnetic susceptibility. There is a simple relationship between the conformation of the trishomocyclopropenylum cation, its charge distribution, and  $\delta^{13}C3$ , which can be used to determine the conformation or the C1C3 interaction distance from NMR measurements. Trishomocyclopropylum cations investigated can rearrange to an envelope form of higher energy where the height of the inversion barrier and the chair-envelope energy difference are a measure for the homoaromatic stabilization energy. The bicyclo[3.1.0]hex-3-yl cation in its envelope form can rearrange with a barrier of just 1 kcal/mol to the bicyclo[3.1.0]hept-2-yl cation. In the case of the bicyclo[3.2.0]hept-3-yl cation, there exists just the envelope form, which can rearrange to a ethano-bridged center-protonated spirocyclopentyl cation. The later cation should be an interesting target of chemical synthesis since it contains a pentacoordinated carbon atom and possesses unusual properties.

## 1. Introduction

The concept of homoaromaticity (HA) was developed in the late fifties by S. Winstein to rationalize the unusual solvolytic behavior of the bicyclo[3.1.0]hex-3-yl cation (**1**).<sup>1</sup> In the last 30 years this concept has been proven to be extremely useful to explain structure, stability, and reactive properties of a large number of compounds as is documented in several review articles.<sup>2–8</sup> Although both experimentalist and theoretician have tried to describe HA compounds in numerous publications, basic properties of HA prototypes such as the homotropylium cation, the cyclobutenyl cation, or cation **1** were unclear for a long time. This has changed only recently as a result of high-quality ab initio calculations that give for the first time precise energy and geometry data for HA compounds. For example, Cremer and co-workers have started a systematic investigation of HA compounds by theoretical means.<sup>9–14</sup> This work is based

on ab initio methods for calculating NMR chemical shifts, which offer a direct link to experimental investigations of HA compounds. The picture which emerges from these investigations partially confirms and partially corrects the definition of HA as it is in the literature.<sup>9–14</sup>

The interacting atoms of a HA compound can be connected by a bond (bond or cyclopropyl HA) or by strong through-space interactions (no-bond HA). The latter case has been found for the homotropylium cation, the 1,4-bishomotropylium cation, and the cyclobutenyl cation. It leads to interesting electronic and structural properties, which can be described in the following way:<sup>9–14</sup>

1. No-bond HA compounds (form B, Scheme 1) possess structures that are intermediate bicyclic (form A) and monocyclic structures (form C) with classical CC bonding. While for A and C the CC interaction distance is either  $<1.6 \text{ \AA}$  or  $>2.4 \text{ \AA}$ , typical interaction distances for a no-bond HA molecule (form B) are in the region 1.8–2.1  $\text{\AA}$ , comparable to CC distances found in transition states (TS) of electrocyclic reactions.<sup>15</sup> As indicated in Scheme 1, HA interactions can occur in a TS of a valence tautomeric reaction between structures A and C. If the TS energy is lowered by HA electron delocalization to a point that form B becomes more stable than either A or C, then the situation of a “frozen TS” will be obtained (Scheme 1).<sup>16</sup> Accordingly, HA equilibrium structures are best viewed as “frozen TSs” that provide insight into TS properties normally not amenable to experiment.

2. For no-bond HA compounds, one calculates a significant increase of the electron density between the

<sup>§</sup> Abstract published in *Advance ACS Abstracts*, March 15, 1996.

(1) (a) Winstein, S.; Sonnenberg, J.; DeVries, L. *J. Am. Chem. Soc.* **1959**, *81*, 6523. (b) Winstein, S. *J. Am. Chem. Soc.* **1959**, *81*, 6524. (c) Winstein, S. *Q. Rev. Chem. Soc.* **1969**, *23*, 141.

(2) Haywood-Farmer, J. *Chem. Rev.* **1974**, *74*, 315.

(3) Paquette, L. A. *Angew. Chem., Int. Ed. Engl.* **1978**, *17*, 106.

(4) Warner, P. M. *Topics in Non-benzoid Aromatic Character*; Hirokawa: Tokyo, 1979; Vol. 2.

(5) Childs, R. F. *Acc. Chem. Res.* **1984**, *17*, 347.

(6) Childs, R. F.; Mahendran, M.; Zeep, S. D.; Shaw, G. S.; Chadda, S. K.; Burke, N. A. D.; George, B. E.; Faggini, R.; Loc, C. J. L. *Pure Appl. Chem.* **1986**, *58*, 111.

(7) Haddon, R. *Acc. Chem. Res.* **1988**, *21*, 243.

(8) Minkin, V. I.; Glukhovtsev, M. N.; Simkin, B. Y. *Aromaticity and Antiaromaticity, Electronic and Structural Aspects*; John Wiley and Sons, Inc.: New York, 1994.

(9) Cremer, D.; Reichel, F.; Kraka, E. *J. Am. Chem. Soc.* **1991**, *113*, 9459.

(10) Svensson, P.; Reichel, F.; Ahlberg, P.; Cremer, D. *J. Chem. Soc., Perkin Trans. 2* **1991**, 1463.

(11) Cremer, D.; Svensson, P.; Kraka, E.; Ahlberg, P. *J. Am. Chem. Soc.* **1993**, *115*, 7445.

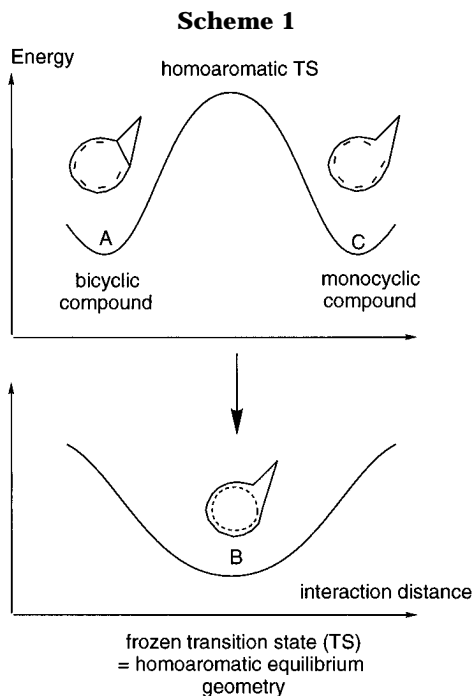
(12) Cremer, D.; Svensson, P.; Kraka, E.; Konkoli, Z.; Ahlberg, P. *J. Am. Chem. Soc.* **1993**, *115*, 7475.

(13) Cremer, D.; Olsson, L.; Kraka, E. *Isr. J. Chem.* **1993**, *33*, 369.

(14) Sieber, S.; Schleyer, P. v. R.; Otto, A. H.; Gauss, J.; Reichel, F.; Cremer, D. *J. Phys. Org. Chem.* **1993**, *6*, 445.

(15) Houk, K. N.; Li, Y.; Evanseck, J. D. *Angew. Chem., Int. Ed. Engl.* **1992**, *31*, 682.

(16) (a) Zimmerman, H. E.; Binkley, R. W.; Givens, R. S.; Grunewald, G. L.; Sherwin, M. A. *J. Am. Chem. Soc.* **1969**, *91*, 3316. (b) Dewar, M. J. S.; Schoeller, W. W. *J. Am. Chem. Soc.* **1971**, *93*, 1481. (c) Hoffmann, R.; Stohrer, W.-D. *J. Am. Chem. Soc.* **1971**, *93*, 6941. (d) Dewar, M. J. S.; Lo, D. H. *J. Am. Chem. Soc.* **1971**, *93*, 7201.



interacting C atoms as a consequence of through-space orbital interactions and electron delocalization. However, there is no indication (e.g., in form of a path of maximum electron density) of the formation of a HA bond.<sup>9</sup>

3. In the cases investigated, a HA stabilization energy (resonance energy) can only be estimated since the HA effect, strain effects, and other electronic effects cannot be segregated. If one takes the classic forms A or C as references (note that in most cases A and C do not correspond to a stationary point and, therefore, the definition of structures A and C is in itself questionable; see second curve in Scheme 1), the extrastabilization of the HA form B can be just a couple of kcal/mol as in the case of the homotropylium cation.<sup>9</sup> However, the bicyclic compound A is already stabilized by cyclopropyl homoconjugation which has to be considered to get the total HA stabilization energy.

4. For the no-bond HA structures investigated so far, bond equalization has been found, although strain effects and nonplanarity of the HA cycle make it difficult exactly to determine the degree of bond equalization. The same holds for CC bond orders obtained from the calculated electron density distribution.

5. In the case of no-bond HA cations, the positive charge is strongly delocalized, which is clearly different from the situation in classical ions where charge is more localized.

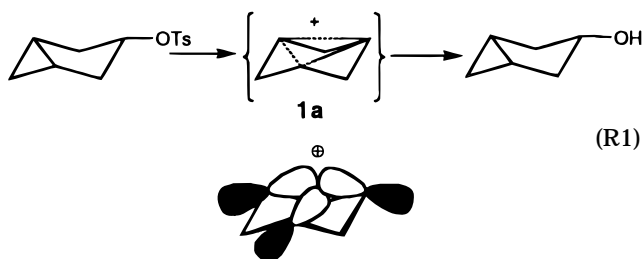
6. <sup>13</sup>C NMR chemical shifts of HA compounds are very sensitive to the degree of charge delocalization in a HA cycle and, therefore, can be used to describe HA compounds. A maximal equalization of chemical shifts normally indicates strong HA interactions.

7. Calculated magnetic susceptibilities of no-bond HA systems without steric constraints, if investigated as a function of the HA interaction distance, reach a maximum value close to 1.9 Å, which seems to be the point of maximum electron delocalization in a HA cycle.

According to this description, HA manifests itself in structure, stability, and magnetic and electronic properties of the compound in question. Of these properties, <sup>13</sup>C chemical shifts are the ones which on the one hand are best to measure and on the other hand are most

sensitive to electronic structure and geometry of a HA compound. The calculation of chemical shifts leads to an ideal connection between experimental and theoretical investigations. Agreement between observed and calculated shift values implies that the electronic state and the geometry used for the shift calculations are similar to those the HA compound possesses under the conditions of the NMR measurement. This can be used for an NMR ab initio determination of geometry and electronic structure as has been shown in previous investigations of mono- and bishomotropylium cations<sup>9–14</sup> and in many other theoretical studies.<sup>17,18</sup>

In this paper, we extend ab initio investigations on mono- and bis-HA compounds to potentially tris-homoaromatic (tris-HA) systems. The prototype of these compounds is the trishomocyclopropenylium cation (**1a**), which was the first HA ion investigated experimentally. Its existence as a reaction intermediate was imposed by Winstein to explain rate enhancement and stereochemistry observed for the hydrolysis of *cis*-bicyclo[3.1.0]hex-3-yl tosylate.<sup>1,19,20</sup> Winstein suggested that in this solvolysis reaction the cyclopropane ring lends anchimeric assistance to heterolytic CO bond cleavage by through-space interactions between the symmetric Walsh orbital  $w_s$  of the cyclopropane ring and the developing  $p\pi(C3)$  orbital.



Many experimental and theoretical studies have confirmed Winstein's hypothesis.<sup>21–27</sup> Cation **1a** was directly observed at low temperatures, and its <sup>1</sup>H and <sup>13</sup>C NMR spectra were measured by several authors.<sup>21–24</sup> Isotope perturbation experiments<sup>23</sup> and analysis of <sup>13</sup>C–<sup>1</sup>H coupling constants<sup>24</sup> verified the existence of the nonclassical cation **1a** rather than static or equilibrating forms of a classical bicyclo[3.1.0]hex-3-yl cation.

(17) See, e.g.: (a) Hnyk, D.; Vajda, E.; Buehl, M.; Schleyer, P. v. R. *Inorg. Chem.* **1992**, *31*, 2464. (b) Buehl, M.; Schleyer, P. v. R. *J. Am. Chem. Soc.* **1992**, *114*, 477. (c) Buehl, M.; Schleyer, P. v. R.; McKee, M. L. *Heteroat. Chem.* **1991**, *2*, 499. (d) Buehl, M.; Schleyer, P. v. R. *Angew. Chem.* **1990**, *102*, 962. (e) Schleyer, P. v. R.; Buehl, M.; Fleischer, U.; Koch, W. *Inorg. Chem.* **1990**, *29*, 153. (f) Schleyer, P. v. R.; Koch, W.; Liu, B.; Fleischer, U. *J. Chem. Soc., Chem. Commun.* **1989**, 1098. (g) Bremer, M.; Schoetz, K.; Schleyer, P. v. R.; Fleischer, U.; Schindler, M.; Kutzelnigg, W.; Koch, W.; Pulay, P. *Angew. Chem.* **1989**, *101*, 1063.

(18) Onak, T.; Tseng, J.; Diaz, M.; Tran, D.; Arias, J.; Herrera, S.; Brown, D. *Inorg. Chem.* **1993**, *32*, 487.

(19) Winstein, S.; Sonnenberg, J. *J. Am. Chem. Soc.* **1961**, *83*, 3235.

(20) Winstein, S.; Fredrich, E. C.; Baker, R.; Lin, Y. *Tetrahedron* **1966**, *Suppl. 8, Part II*, 621.

(21) Masamune, S.; Sakai, M.; Kemp-Jones, A. V.; Nakashima, T. *Can. J. Chem.* **1974**, *52*, 855. Masamune, S.; Sakai, M.; Kemp-Jones, A. V. *Can. J. Chem.* **1974**, *52*, 858.

(22) Olah, G. A.; Prakash, G. K. S.; Rawdah, T. N.; Whittaker, D. W.; Rees, J. C. *J. Am. Chem. Soc.* **1979**, *101*, 3935.

(23) Prakash, G. K. S.; Arvanaghi, M.; Olah, G. A. *J. Am. Chem. Soc.* **1985**, *107*, 6017.

(24) Kelly, D. P.; Giansiracusa, J. J.; Leslie, D. R.; McKern, I. D.; Sinclair, G. S. *J. Org. Chem.* **1988**, *53*, 2497.

(25) Jorgensen, W. L. *Tetrahedron Lett.* **1976**, *35*, 3029.

(26) Buzek, P.; Schleyer, P. v. R.; Sieber, S. *Chem. Unserer Zeit* **1992**, *26*, 116.

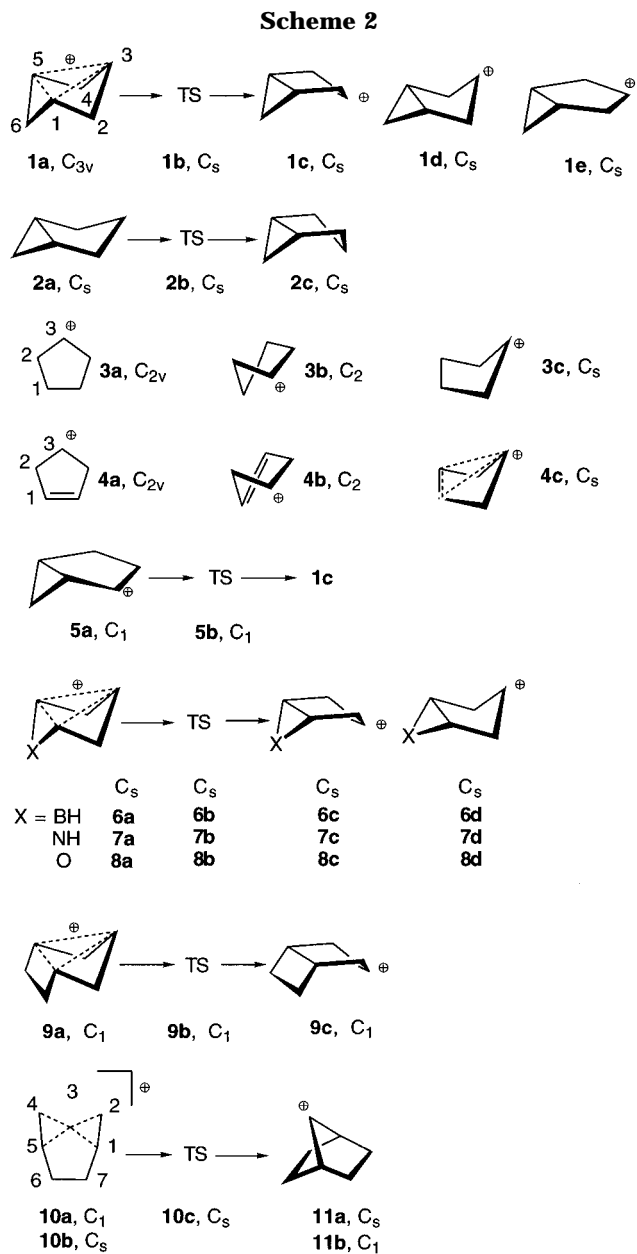
(27) Mjoberg, P. J.; Almöf, J. *Chem. Phys.* **1978**, *29*, 201.

MINDO/3 calculations of Jørgensen<sup>25</sup> and ab initio calculations of Buzek and co-workers<sup>26</sup> both confirmed that **1** possesses  $C_{3v}$  symmetry and corresponds to a minimum on the potential energy surface (PES). Buzek and co-workers have also reported IGLO chemical shifts in good agreement with measured shift data,<sup>21–24</sup> which adds further credibility to their structural calculations. According to Jørgensen's semiempirical results, the classical cation is also a minimum on the PES, but less stable than **1a** by 12.6 kcal/mol. In an early ab initio investigation of **1**, Mjöberg and Almlöf<sup>27</sup> suggested that the classical rather than the nonclassical cation corresponds to the global energy minimum on the PES.

Although the intermediary of **1a** in solvolysis reactions such as (1) has been proven, a number of questions concerning, for example, the formation of trishomocyclopropenylum cations, their stabilization in dependence on conformation and substituents, the degree of HA electron delocalization, and their rearrangement possibilities are not clear. For example, there is experimental evidence that suggests that bicyclo[3.1.0]hexane (**2**) and its derivatives prefer a boat form<sup>28–33</sup> while **1** should be most stable in a chair conformation. Obviously, a conformational process must precede or accompany the actual solvolysis reaction; otherwise anchimeric assistance in solvolysis is not possible. Therefore, the conformational flexibility of both **2** and cation **1** have to be known to understand the rate acceleration data collected in experimental studies.

In this work, the following questions are discussed: (1) What conformational and stereoelectronic requirements have to be fulfilled to have the most effective through-space orbital interactions in trishomocyclopropenylum cations? (2) At which stage of the solvolysis reaction do through-space interactions develop? What steps precede the formation of the intermediate **1a**? (3) How does remote perturbation caused by a heteroatom in position 6 influence through-space interactions and HA of trishomocyclopropenylum cations? (4) Does a HA bicyclo[3.2.0]hept-3-yl cation exist and how effective is the cyclobutane ring in through-space interactions? (5) What predictions can be made for solvolysis reactions of bicyclo[3.1.0]hex-3-yl derivatives, in particular, in the case of 6-hetero-substituted compounds? (6) Does trishomoaromaticity differ in any way from mono- or bishomoaromaticity? (7) Does the investigation of trishomoaromaticity lead to the suggestion of new unusual chemical compounds with nonclassical bonding patterns?

The present investigation is carried out in a similar way as in the case of mono- and bishomotropylium cations.<sup>9,12</sup> First we explore the PES of cation **1** in the direction of the homoaromatic interaction distance C1C3 in order to determine the position of global and possible local energy minima on the PES. We extend this search also in the direction of possible chair–boat interconversion modes to see whether both forms can exist under experimental conditions. For comparison, we also investigate possible boat–chair interconversions in the case of the neutral molecule **2**. These calculations help to



elucidate the mechanism of the formation of **1a** in a solvolysis reaction.

In addition to molecules **1** and **2**, we investigate the cyclopentyl (**3**), the cyclopenten-4-yl cation (**4**), and the bicyclo[3.1.0]hex-2-yl cation (**5**), which are suitable reference compounds (see Scheme 2). Finally, we study how insertion of a heteroatom into the cyclopropane unit or an enlargement of the cyclopropane to a cyclobutane ring affects HA interactions in **1**. For this purpose, we calculate three 6-X-bicyclo[3.1.0]hex-3-yl (X = BH (**6**), NH (**7**), O (**8**)) cations and the bicyclo[3.2.0]hept-3-yl cation (**9**). The latter compound is interesting since, if it exists, it can rearrange to isomeric forms, of which cation **10** and the norbornyl cation **11** shown in Scheme 2 are also discussed in this work.

## 2. Computational Methods

Various forms of molecules **1–10** (see Scheme 2) have been fully optimized employing Hartree–Fock (HF) and second-order Møller–Plesset (MP2) perturbation theory<sup>34</sup> in connection with the 6-31G(d) basis set,<sup>35</sup> which is of DZ+P quality in the valence shell. Harmonic frequencies have been calcu-

(28) Lord, R. C.; Malloy, T. B. *J. Mol. Spectrosc.* **1973**, *46*, 358.

(29) Cook, R. L.; Malloy, T. B. *J. Am. Chem. Soc.* **1974**, *96*, 1703.

(30) Lewis, J. D.; Laane, J. *J. Chem. Phys.* **1974**, *61*, 2342.

(31) Mastryukov, V. S.; Osina, E. L.; Vilkov, L. V.; Hildebrandt, R. L. *J. Am. Chem. Soc.* **1977**, *99*, 6855.

(32) Rees, J. C.; Whittaker, D. *Org. Magn. Reson.* **1981**, *15*, 363.

(33) Traetteberg, M.; Bakken, P.; Seip, R.; Whittaker, D. *J. Mol. Struct.* **1984**, *116*, 119.

(34) Hariharan, P. C.; Pople, J. A. *Theor. Chim. Acta* **1973**, *28*, 213.

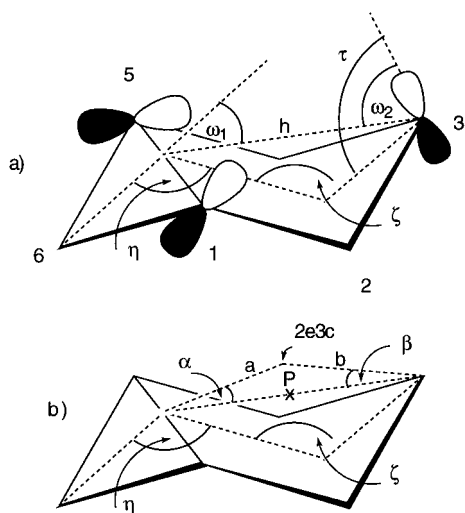


**Figure 1.** (a) Definition of folding angles  $\eta$  and  $\zeta$ , orbital inclination angles  $\omega_1$  and  $\omega_2$ , and the pyramidalization angle  $\tau$  for cation **1**. In the case of  $\omega_1$ , it is assumed that the symmetric Walsh orbital  $w_s$  lies in the plane of the cyclopropane ring. Angles  $\omega_2$  and  $\tau$  are defined by assuming that the  $p\pi(C3)$  orbital is directed along a local  $C_3$  axis. (b) Parameters  $a$ ,  $b$ ,  $\alpha$ , and  $\beta$  determine the position (centroid of charge) of the two-electron, three-center (2e3c) LMO of **1a** above the plane C1C3C5.

lated in all cases at the HF/6-31G(d) level and in selected cases also at the MP2/6-31G(d) level in order to characterize calculated stationary points and to determine zero-point energies (ZPE). Single-point calculations with MP2/6-31G(d) geometries have been carried out at higher levels of theory, namely, at third-order MP (MP3) and fourth-order MP (MP4) theory where in the later case single (S), double (D), and quadruple (Q) excitations have been included (MP4(SDQ)).<sup>34</sup> These calculations are denoted by MP3/6-31G(d)//MP2/6-31G(d) and MP4(SDQ)/6-31G(d)//MP2/6-31G(d).

NMR chemical shift calculations have been carried out with the IGLO (individual gauge for localized orbitals) method of Kutzelnigg and Schindler<sup>36–38</sup> in a version<sup>39</sup> designed for routine calculations with the programs COLOGNE94<sup>40</sup> and GAUSSIAN92.<sup>41</sup> Although IGLO calculations normally require TZ+P basis sets for most nuclei, we have used the 6-31G(d) basis set throughout to get <sup>13</sup>C NMR chemical shifts. Previous investigations have shown that IGLO/6-31G(d) leads to reasonable  $\delta^{13}\text{C}$  values.<sup>9,39</sup>

### 3. Structure and Stability of the Trishomocyclopropylm Cation

Figure 1 gives some geometrical parameters of the bicyclo[3.1.0]hexyl ring which are useful for the discussion of its conformation and stereoelectronic properties. These are the folding angles  $\eta$  and  $\zeta$ , the orbital inclination angles  $\omega_1$  and  $\omega_2$ , and the pyramidalization angle  $\tau$  (Figure 1a). Other geometrical parameters ( $a$ ,  $b$ ,  $\alpha$  and

$\beta$ ) defined in Figure 1b describe the location of the centroid of a (localized) two-electron, three-center (2e3c) orbital characteristic of **1** and related cations.

HF and MP2 geometrical parameters of molecules **1–10** calculated in this work are summarized in Table 1 (Cartesian coordinates of all optimized geometries are summarized in the supporting information). The corresponding energies are given in Table 2. In Table 3, IGLO chemical shifts and orbital contributions to the absolute <sup>13</sup>C chemical shift of C3,  $\sigma(C3)$ , are given. Mulliken charges are listed in Table 4.

**Equilibrium Geometry.** The geometries calculated for **1a** at the HF/6-31G(d) and MP2/6-31G(d) level of theory are very similar (Table 1) and agree with data published by Buzek and co-workers.<sup>26</sup> Both methods predict that the cation possesses  $C_{3v}$  symmetry with interaction distances C1C3 = C1C5 = C3C5 = 1.82 Å. This value is confirmed at the MP3/- and MP4(SDQ)/6-31G(d) levels of theory, which lead to the same C1C5 value and the same curvature close to the minimum. The calculated (harmonic) C1C5 stretching constant is 1.03 mdyn/Å at MP4(SDQ)/6-31G(d), which is relatively large compared to the (harmonic) C1C7 stretching constant of the 1,7-monohomotropylium cation (0.2 mdyn/Å at MP4(SDQ)/6-31G(d)<sup>9</sup>), but still small compared to the stretching constant of a normal CC bond (5 mdyn/Å<sup>42</sup>). This means that HA interactions stabilize **1a** considerably, and as a consequence, the equilibrium geometry of **1a** will not be perturbed so easily as it is in the case for monohomotropylium cations.<sup>43</sup>

A  $C_{3v}$ -symmetrical distortion of **1a** leading to C1C3 = C1C5 = C3C5 = 2.4 Å increases the relative energy to 65 kcal/mol, thus reflecting the fact that at such a distance a CC bond has been lost and through-space interactions between centers C1, C3, and C5 are not effective because of small overlap. The C1C3C5 breathing force constant is 3.59 mdyn/Å, which indicates that the geometry of **1a** is relatively rigid.

In view of the fact that all experimental information on **1a** was obtained in solution, we have made a third check on the equilibrium geometry of **1a** by comparing calculated IGLO <sup>13</sup>C NMR chemical shifts for **1a** with the corresponding experimental values measured in solution. Calculated shift values are sensitive to the geometry used in the calculation and, therefore, the deviations  $\Delta$  between experimental and theoretical shift values also reflect inconsistencies between calculated and true equilibrium geometry. If the mean deviation of the calculated <sup>13</sup>C chemical shift values is plotted against the distance C1C5 (Figure 2), then a parabola results with its minimum at 1.82 Å. At this point calculated and experimental shift values differ by 3.1 ppm, thus showing that the calculated equilibrium geometry indeed provides the best agreement between experimental and calculated shift values. This suggests that the gas phase geometry of **1a** is also valid in solution.

The conformation of **1a** corresponds to a chair with two different folding angles  $\eta$  (117°, MP2/6-31G(d), Table 1) and  $\zeta$  (87°) where the latter value is a consequence of the relatively short 1,3 interaction distances (bond angle

(35) Pople, J. A.; Binkley, J. S.; Seeger, R. *Int. J. Quantum Chem. Symp.* **1976**, *10*, 1. Krishnan, R.; Pople, J. A. *Int. J. Quantum Chem.* **1978**, *14*, 91.

(36) Kutzelnigg, W. *Isr. J. Chem.* **1980**, *19*, 193.

(37) Schindler, M.; Kutzelnigg, W. *J. Chem. Phys.* **1982**, *76*, 1919.

(38) Kutzelnigg, W.; Schindler, M.; Fleischer, U. *NMR, Basic Principles and Progress*; Springer: Berlin, 1989; Vol. 23, p 2.

(39) Reichel, F. Thesis, University of Köln, 1991.

(40) Gauss, J.; Kraka, E.; Reichel, F.; Olsson, L.; Zhe He; Cremer, D. COLOGNE94, Göteborg, 1993.

(41) Frisch, M. J.; Head-Gordon, M.; Trucks, G. W.; Foresman, J. B.; Schlegel, H. B.; Raghavachari, K.; Robb, M. A.; Binkley, J. S.; Gonzales, C.; Defrees, D. J.; Fox, D. J.; Whiteside, R. A.; Seeger, R.; Melius, C. F.; Baker, J.; Martin, R. L.; Kahn, L. R.; Stewart, J. J. P.; Topiol, S.; Popole, J. A. GAUSSIAN92, Pittsburgh, 1992.

(42) Shimanouchi, T. The Molecular Force Field. In *Physical Chemistry: An Advanced Treatise*, Vol. IV; Eyring, H., Henderson, D., Yost, W., Eds.; Academic Press: New York, 1970.

(43) Cremer, D.; Svensson, P., unpublished results.

(44) Schindler, M. *J. Am. Chem. Soc.* **1987**, *109*, 1020.

(45) Schleyer, P. v. R.; Carneiro, J. W. d. M. *J. Am. Chem. Soc.* **1989**, *111*, 5475.

Table 1. Selected Geometrical Parameters of Molecules 1–10<sup>a</sup>

compd	sym	C1C2	C2C3	C1X6	C1C5	C1C3	∠ <sub>561</sub>	∠ <sub>123</sub>	∠ <sub>234</sub>	η	ζ
<b>1a</b>	C <sub>3v</sub>	1.483	1.483	1.483	1.821	1.821	75.8	75.8	121.0	119.9	87.3
		<i>1.485</i>	<i>1.485</i>	<i>1.485</i>	<i>1.824</i>	<i>1.824</i>	<i>75.8</i>	<i>75.8</i>	<i>120.5</i>	<i>117.4</i>	<i>87.1</i>
<b>1b</b>	C <sub>s</sub>	1.539	1.478	1.490	1.538	2.265	62.1	97.3	114.4	112.1	138.5
		<i>1.533</i>	<i>1.461</i>	<i>1.494</i>	<i>1.545</i>	<i>2.278</i>	<i>62.3</i>	<i>99.0</i>	<i>115.3</i>	<i>112.0</i>	<i>143.8</i>
<b>1c</b>	C <sub>s</sub>	1.521	1.464	1.495	1.511	2.372	60.7	105.3	113.2	110.5	187.9
		<i>1.511</i>	<i>1.444</i>	<i>1.500</i>	<i>1.523</i>	<i>2.363</i>	<i>61.0</i>	<i>106.1</i>	<i>112.9</i>	<i>109.8</i>	<i>189.2</i>
<b>1d</b>	C <sub>s</sub>	1.533	1.461	1.473	1.500	1.899	61.2	78.7	120.2	113.1	101.2
		<i>1.526</i>	<i>1.464</i>	<i>1.474</i>	<i>1.500</i>	<i>1.829</i>	<i>61.2</i>	<i>75.4</i>	<i>120.6</i>	<i>113.1</i>	<i>95.5</i>
<b>2a</b>	C <sub>s</sub>	1.529	1.543	1.498	1.503	2.435	60.3	104.9	106.2	111.6	152.8
		<i>1.524</i>	<i>1.538</i>	<i>1.502</i>	<i>1.513</i>	<i>2.419</i>	<i>60.5</i>	<i>104.4</i>	<i>104.9</i>	<i>111.6</i>	<i>147.4</i>
<b>2b</b>	C <sub>s</sub>	1.525	1.550	1.498	1.501	2.457	60.1	106.1	107.6	110.7	166.6
		<i>1.519</i>	<i>1.549</i>	<i>1.502</i>	<i>1.508</i>	<i>2.455</i>	<i>60.3</i>	<i>106.3</i>	<i>107.9</i>	<i>110.1</i>	<i>169.4</i>
<b>2c</b>	C <sub>s</sub>	1.520	1.542	1.500	1.501	2.427	60.1	104.9	105.3	112.0	208.8
		<i>1.515</i>	<i>1.538</i>	<i>1.504</i>	<i>1.509</i>	<i>2.415</i>	<i>60.2</i>	<i>104.5</i>	<i>105.0</i>	<i>111.8</i>	<i>211.4</i>
exp <sup>b</sup>		1.530	1.530	1.513	1.513	2.358	60.0	100.8	108.6	117.0	218.0
exp <sup>c</sup>		1.543	1.543	1.515	1.454	2.415	57.3	103.0	108.2	109.4	205.2
<b>3a</b>	C <sub>2v</sub>	1.545	1.456		1.555	2.407		106.6	113.6		180.0
		<i>1.538</i>	<i>1.438</i>		<i>1.554</i>	<i>2.395</i>		<i>107.1</i>	<i>113.7</i>		<i>180.0</i>
<b>3b</b>	C <sub>2</sub>	1.542	1.457		1.539	2.381		105.3	111.9		180.0
		<i>1.538</i>	<i>1.439</i>		<i>1.534</i>	<i>2.372</i>		<i>105.7</i>	<i>111.5</i>		<i>180.0</i>
<b>4a<sup>d</sup></b>	C <sub>2v</sub>	1.511	1.463		1.319	2.330		103.1	111.2		180.0
		<i>1.500</i>	<i>1.442</i>		<i>1.344</i>	<i>2.330</i>		<i>104.9</i>	<i>110.3</i>		<i>180.0</i>
<b>4c<sup>d</sup></b>	C <sub>s</sub>	1.495	1.488		1.369	1.813		74.8	110.6		93.8
		<i>1.484</i>	<i>1.502</i>		<i>1.395</i>	<i>1.760</i>		<i>72.2</i>	<i>109.8</i>		<i>88.7</i>
<b>5a</b>	C <sub>1</sub>	1.361	1.497	1.603	1.685	2.427	67.6	116.2	104.2	109.9	199.8
		<i>1.364</i>	<i>1.490</i>	<i>1.605</i>	<i>1.694</i>	<i>2.419</i>	<i>67.8</i>	<i>115.8</i>	<i>104.6</i>	<i>108.6</i>	<i>198.8</i>
<b>5b</b>	C <sub>1</sub>	1.497	1.394	1.502	1.515	2.367	60.8	109.9	111.9	110.5	190.8
		<i>1.500</i>	<i>1.419</i>	<i>1.502</i>	<i>1.525</i>	<i>2.366</i>	<i>61.1</i>	<i>109.7</i>	<i>112.2</i>	<i>109.7</i>	<i>190.6</i>
<b>6a</b>	C <sub>s</sub>	1.482	1.486	1.539	2.010	1.838	81.5	76.5	119.3	126.8	81.7
		<i>1.489</i>	<i>1.483</i>	<i>1.530</i>	<i>1.995</i>	<i>1.851</i>	<i>81.4</i>	<i>77.0</i>	<i>118.4</i>	<i>127.7</i>	<i>82.6</i>
<b>6b</b>	C <sub>s</sub>	1.543	1.477	1.539	1.584	2.283	61.9	98.1	114.0	114.6	137.6
		<i>1.539</i>	<i>1.460</i>	<i>1.537</i>	<i>1.589</i>	<i>2.288</i>	<i>62.3</i>	<i>99.4</i>	<i>115.2</i>	<i>113.7</i>	<i>141.8</i>
<b>6c</b>	C <sub>s</sub>	1.529	1.461	1.541	1.558	2.389	60.7	106.1	113.8	115.3	184.2
		<i>1.520</i>	<i>1.441</i>	<i>1.538</i>	<i>1.571</i>	<i>2.382</i>	<i>61.4</i>	<i>107.1</i>	<i>113.3</i>	<i>115.4</i>	<i>187.4</i>
<b>7a, ax</b>	C <sub>s</sub>	1.491	1.480	1.405	1.745	1.834	76.8	76.3	120.4	117.3	90.3
<b>7b, eq</b>	C <sub>s</sub>	1.498	1.491	1.418	1.737	1.858	75.5	77.2	120.1	117.1	92.1
		<i>1.543</i>	<i>1.479</i>	<i>1.433</i>	<i>1.507</i>	<i>2.214</i>	<i>63.4</i>	<i>94.2</i>	<i>116.2</i>	<i>104.5</i>	<i>134.4</i>
<b>7c, eq</b>	C <sub>s</sub>	1.542	1.462	1.457	1.512	2.239	62.5	96.3	116.8	103.8	140.1
		<i>1.516</i>	<i>1.469</i>	<i>1.440</i>	<i>1.478</i>	<i>2.346</i>	<i>61.6</i>	<i>103.6</i>	<i>113.5</i>	<i>101.9</i>	<i>193.5</i>
<b>8a</b>	C <sub>s</sub>	1.508	1.450	1.468	1.492	2.337	61.1	104.4	113.5	100.7	193.6
		<i>1.480</i>	<i>1.489</i>	<i>1.365</i>	<i>1.702</i>	<i>1.809</i>	<i>77.1</i>	<i>75.1</i>	<i>120.2</i>	<i>110.9</i>	<i>90.1</i>
<b>8b</b>	C <sub>s</sub>	1.485	1.488	1.346	1.706	1.817	75.4	75.4	120.4	110.3	90.4
		<i>1.549</i>	<i>1.475</i>	<i>1.383</i>	<i>1.480</i>	<i>2.217</i>	<i>64.7</i>	<i>94.3</i>	<i>116.3</i>	<i>103.7</i>	<i>135.6</i>
<b>8c</b>	C <sub>s</sub>	1.554	1.457	1.417	1.483	2.288	63.1	97.2	117.1	103.7	144.1
		<i>1.517</i>	<i>1.469</i>	<i>1.400</i>	<i>1.458</i>	<i>2.348</i>	<i>62.8</i>	<i>103.6</i>	<i>113.4</i>	<i>102.2</i>	<i>190.4</i>
<b>9a</b>	C <sub>1</sub>	1.511	1.449	1.438	1.473	2.341	61.7	104.5	113.5	101.8	189.2
		<i>1.563</i>	<i>1.456</i>	<i>1.544<sup>e</sup></i>	<i>1.646</i>	<i>2.010</i>	<i>91.7<sup>f</sup></i>	<i>83.4</i>	<i>121.1</i>	<i>117.4</i>	<i>113.1</i>
<b>9b</b>	C <sub>1</sub>	1.576	1.457	1.548 <sup>e</sup>	1.577	2.185	89.9 <sup>f</sup>	92.1	115.3	119.5	147.1
		<i>1.533</i>	<i>1.458</i>	<i>1.550<sup>e</sup></i>	<i>1.557</i>	<i>2.377</i>	<i>89.1<sup>f</sup></i>	<i>105.2</i>	<i>113.4</i>	<i>116.0</i>	<i>199.2</i>
<b>9c</b>	C <sub>1</sub>	1.526	1.440	1.550 <sup>e</sup>	1.556	2.365	88.6 <sup>f</sup>	105.8	112.8	115.0	206.1
		<i>1.416</i>	<i>1.609</i>	<i>1.522<sup>e</sup></i>	<i>2.442</i>	<i>1.649</i>	<i>104.5<sup>f</sup></i>	<i>65.7</i>	<i>113.6</i>		
<b>10a</b>	C <sub>1</sub>	1.428	1.617	1.519 <sup>e</sup>	2.432	1.622	103.9 <sup>f</sup>	64.0	111.6		
		<i>1.420</i>	<i>1.589</i>	<i>1.524<sup>e</sup></i>	<i>2.442</i>	<i>1.655</i>	<i>107.2<sup>f</sup></i>	<i>66.5</i>	<i>112.9</i>		
<b>10b</b>	C <sub>s</sub>	1.432	1.594	1.520 <sup>e</sup>	2.433	1.628	107.0 <sup>f</sup>	64.8	110.3		
		<i>1.485</i>	<i>1.804</i>	<i>1.563<sup>e</sup></i>	<i>2.451</i>	<i>1.477</i>	<i>106.8<sup>f</sup></i>	<i>52.3</i>	<i>69.7</i>		
<b>10c</b>	C <sub>s</sub>	1.491	1.787	1.562 <sup>e</sup>	2.450	1.477	106.9 <sup>f</sup>	52.6	68.8		

<sup>a</sup> Distances in Å and angles in deg. For the definition of folding angles η and ζ, see Figure 1. First entry (normal print) gives HF/6-31G(d) values, second entry (italic print) gives MP2/6-31G(d) values. <sup>b</sup> Experimental geometry from ref 29. <sup>c</sup> Experimental geometry from ref 31. <sup>d</sup> HF/6-31G(d) geometry from ref 47. <sup>e</sup> Distance C1C7. <sup>f</sup> Angle C6C7C1 = ∠<sub>671</sub>.

C1C2C3 = 75.8°). One only needs the folding angle η, which measures the bending of the CH<sub>2</sub> groups out of the plane of the three CH groups, to describe the conformation of **1a**. But we will continue to use the chair description since the preferred conformational process of **1a** is its interconversion into a boat form and for this process the angle ζ is the appropriate conformational parameter.

Experimental and IGLO/6-31G(d) <sup>13</sup>C chemical shifts (Table 3, Figure 2) agree very well and suggest that gas phase and solution phase shifts do not differ very much.

Compared to the chemical shifts of a normal carbocation such as the cyclopentyl cation (**3**), the shift values of **1a** differ very much. Since positive charge is equally spread over three CH groups and, in addition, delocalized onto the neighboring CH<sub>2</sub> groups by hyperconjugation, C1H, C3H, and C5H carry a much smaller positive charge (0.1 electron, Table 4) and are much more shielded than for example the CH<sup>+</sup> group in **3** (0.5 e). As a consequence, their shift value (0.9; expt 4.7, Table 3) appears 360 ppm upfield compared to that of the C<sup>+</sup> atom of the planar form **3a** (363.9 ppm).

**Table 2. Absolute and Relative Energies of Molecule 1–11<sup>a</sup>**

compd	sym	HF/6-31G(d) //HF/6-31G(d)			MP2/6-31G(d) //MP2/6-31G(d)			MP3/6-31G(d) //MP2/6-31G(d)			MP4SDQ/6-31G(d) //MP2/6-31G(d)		
		<i>E</i>	$\Delta E$	ZPE	<i>E</i>	$\Delta E$	<i>E</i>	$\Delta E$	<i>E</i>	$\Delta E$	<i>E</i>	$\Delta E$	$\Delta E + \text{ZPE}$
<b>1a</b>	C <sub>3v</sub>	-232.14158 (0)	0	77.7	-232.93862	0	-232.97583	0	-232.98499	0	0		
<b>1b</b>	C <sub>s</sub>	-232.11132 (1)	19.0	77.1	-232.88684	32.5	-232.93326	26.7	-232.94351	26.0	25.4		
<b>1c</b>	C <sub>s</sub>	-232.12441 (0)	10.8	77.1	-232.90051	23.9	-232.94697	18.1	-232.95719	17.4	16.8		
<b>1d</b>	C <sub>s</sub>	-232.12372 (ns)	11.2		-232.91799	12.9	-232.95611	12.4	-232.96551	12.2			
<b>1e</b>	C <sub>s</sub>	-232.12396 (ns)	11.1		-232.89979	24.4	-232.94645	18.4	-232.95662	12.6			
<b>5a</b>	C <sub>1</sub>	-232.15319 (0)	-7.3	78.4	-232.93795	0.4	-232.98054	-3.0	-232.98994	-3.1	-2.4		
<b>5b</b>	C <sub>1</sub>	-232.11713 (1)	15.3	76.8	-232.89975	24.4	-232.94539	19.1	-232.95543	18.5	17.6		
<b>2a</b>	C <sub>s</sub>	-232.99563 (0)	0	85.8	-233.80495	0	-233.85177	0	-233.86163	0	0		
<b>2b</b>	C <sub>s</sub>	-232.99538 (1)	0.2	85.7	-233.80375	0.8	-233.85104	0.5	-233.86086	0.5	0.4		
<b>2c</b>	C <sub>s</sub>	-233.00107 (0)	-3.4	86.0	-233.81079	-3.7	-233.85734	-3.5	-233.86731	-3.6	-3.4		
<b>3a</b>	C <sub>2v</sub>	-194.28869 (1)	0		-194.93239	0	-194.97907	0	-194.98870	0			
<b>3b</b>	C <sub>2</sub>	-194.29284 (0)	-2.6		-194.93824	-3.7	-194.98379	-3.0	-194.99339	-2.9			
<b>4a</b>	C <sub>2v</sub>	-193.09737 (1)	0	53.6	-193.73155	0	-193.77101	0	-193.78046	0	0		
<b>4c</b>	C <sub>s</sub>	-193.10121 (0)	-2.4	55.1	-193.75130	-12.4	-193.78313	-7.6	-193.79008	-6.0	-4.5		
<b>6a</b>	C <sub>s</sub>	-218.34982 (0)	0	68.9	-219.08488	0	-219.12255	0	-219.13153	0	0		
<b>6b</b>	C <sub>s</sub>	-218.31157 (1)	24.0	67.0	-219.02499	37.6	-219.07174	31.8	-219.08169	31.2	29.3		
<b>6c</b>	C <sub>s</sub>	-218.32195 (0)	17.5	66.9	-219.03705	30.0	-219.08376	24.3	-219.09369	23.7	21.7		
<b>6d</b>	C <sub>s</sub>	-218.32644 (ns)	14.7										
<b>7a, ax</b>	C <sub>s</sub>	-248.11321 (0)	0	72.7	-248.94208	0	-248.97294	0	-248.98282	0	0		
<b>7a, eq</b>	C <sub>s</sub>	-248.10914	2.6		-248.93625	3.7	-248.96831	2.9	-248.97754	3.3			
<b>7a, pl</b>	C <sub>s</sub>	-248.09255 (1)	13.0	70.7	-248.91950	14.2	-248.95087	13.8	-248.96028	14.2	12.7		
<b>7b, ax</b>	C <sub>s</sub>	-248.08747	16.2										
<b>7b, eq</b>	C <sub>s</sub>	-248.09035 (1)	14.4	70.4	-248.89797	27.7	-248.93837	21.7	-248.94900	21.2	19.4		
<b>7c, ax</b>	C <sub>s</sub>	-248.09582	10.9										
<b>7c, eq</b>	C <sub>s</sub>	-248.11006 (0)	2.0	70.9	-248.91609	16.3	-248.95689	10.1	-248.96772	9.5	8.2		
<b>7d, ax</b>	C <sub>s</sub>	-248.09936 (ns)	8.7										
<b>7d, eq</b>	C <sub>s</sub>	-248.09566 (ns)	11.0										
<b>8a</b>	C <sub>s</sub>	-267.92607 (0)	0	64.9	-268.76621	0	-268.79184	0	-268.80317	0	0		
<b>8b</b>	C <sub>s</sub>	-267.91319 (1)	8.1	63.2	-268.73639	18.7	-268.76915	14.2	-268.78327	12.5	10.8		
<b>8c</b>	C <sub>s</sub>	-267.93014 (0)	-2.6	63.3	-268.74935	10.6	-268.78324	5.3	-268.79638	4.3	2.7		
<b>8d</b>	C <sub>s</sub>	-267.91724 (ns)	5.5										
<b>9a</b>	C <sub>1</sub>	-271.15177 (0)	0		no stationary point found								
<b>9b</b>	C <sub>1</sub>	-271.15071 (1)	0.7	95.1	no stationary point found								
<b>9c</b>	C <sub>1</sub>	-271.16586 (0)	-8.8	94.5	-272.07953		-272.13538		-272.14759				
<b>10a</b>	C <sub>1</sub>	-271.17305 (0)	0	96.0	-272.10784 (0)	0	-272.15528	0	-272.16594	0	0		
<b>10b</b>	C <sub>s</sub>	-271.17073 (1)	1.5	95.9	-272.10414 (1)	2.3	-272.15238	1.8	-272.16281	2.0	1.9		
<b>10c</b>	C <sub>s</sub>	-271.14539 (1)	17.4	95.5	-272.08093 (1)	16.9	-272.12858	16.8	-272.13980	16.4	15.9		
<b>11a</b>	C <sub>s</sub>	-271.17766 (0)	-2.9	96.0	-272.09709 (1)	6.7	-272.14926	3.8	-272.16122	3.0	3.0		
<b>11b</b>	C <sub>1</sub>	-271.17415 (1)	-2.2	96.1	-272.10456 (0)	2.1	-272.15543	-0.1	-272.16620	-0.2	-0.1		

<sup>a</sup> Absolute energies in hartrees, relative energies and zero-point energies (ZPEs) in kcal/mol. Numbers in parentheses give the number of imaginary frequencies; ns denotes a nonstationary point. Abbreviations ax, eq, or pl indicate that the NH bond is in an axial, equatorial, or intermediate (TS for inversion at N) position. The ZPEs are calculated at the HF/6-31G(d) level of theory and are scaled by 0.87. Calculations for **11a** and **11b** from ref 60.

**Homoaromatic Stabilization Energy.** The determination of a HA stabilization energy always implies the definition of an appropriate reference molecule or reference form. A possible reference form might be a form of the cation in which through-space interactions are strongly reduced or even excluded. For example, freezing the C1C5 distance to the value one would expect for a cyclopropane ring (1.500 Å, MP2/6-31G(d)<sup>46</sup>) and reoptimizing all other parameters leads to form **1d** (Scheme 2), which possesses slightly increased 1,3 distances (1.830 Å, MP2/6-31G(d), Table 1) and a larger folding angle  $\zeta$  (95°). The energy of **1d** is 12 kcal/mol (MP4(SDQ)//MP2, Table 2) higher than that of **1a**. Shift values ( $\delta^{13}\text{C}3 = 109$  ppm, Table 3) and calculated charges suggest reduced but still substantial HA interactions. This confirms that even a normal cyclopropane ring strongly interacts with C3<sup>+</sup> and that the HA stabilization energy must be considerably larger than  $E(\mathbf{1d}) - E(\mathbf{1a}) = 12$  kcal/mol.

An alternative choice of an appropriate reference for **1a** is the cyclopenten-4-yl cation (**4**). If **4** folds to an envelope conformation (**4c**, Scheme 2), the  $\pi$ -orbitals of the double bond can interact with the empty  $p\pi$  orbital at C<sup>+</sup> and by delocalization of the  $\pi$ -electrons of the double bond a bis-HA system is formed. Schleyer and co-workers<sup>47</sup> calculated for this cation a strongly folded envelope form **4c** ( $\zeta = 94^\circ$ ) at the HF/6-31G(d) level of theory. For comparison, the envelope form **3c** of the cyclopentyl cation (Scheme 2), when optimized, rearranges to the planar form **3a**. The latter form guarantees a larger CC<sup>+</sup>C angle and, in particular, optimal hyperconjugative interactions between C<sup>+</sup> and the adjacent CH<sub>2</sub> groups. However, the equilibrium geometry of **3** corresponds to the twist form **3b** which is 2.9 kcal/mol (MP4(SDQ)//MP2, Table 2) more stable than **3a** because of a reduction of eclipsing strain that dominates changes in angle strain and hyperconjugative stabilization. The

(46) Cremer, D.; Kraka, E. *J. Am. Chem. Soc.* **1985**, *107*, 3800.

(47) Schleyer, P. v. R.; Bentley, T. W.; Koch, W.; Kos, A. J.; Schwarz, H. *J. Am. Chem. Soc.* **1987**, *109*, 6953.

(48) In the case of  $\omega_1$ , we have assumed that the Walsh orbitals of the three-membered ring are in the plane of the ring; in the case of  $\omega_2$ , we have assumed local C<sub>3v</sub> symmetry at C3 with the  $p\pi$  orbital pointing along the C<sub>3</sub> axis. See, Figure 1.

Table 3. IGLO Chemical Shifts<sup>a</sup> and Magnetic Susceptibilities for Molecules 1–10

compd	sym	X6	$\delta$ (ppm) on atom				LMO contributions to $\sigma(C3)$				$-\chi$	$\delta^1H(C3)$
			C1	C2	C3	X6	2e3c	C2C3	C3H3	<i>P</i>		
<b>1a</b>	<i>C</i> <sub>3v</sub>	CH <sub>2</sub>	0.9 4.7 <sup>b</sup>	15.7 17.3 <sup>b</sup>	0.9 4.7 <sup>b</sup>	15.7 17.3 <sup>b</sup>	+25.0	+8.1	+1.6	1.000	81.3	0.9
<b>1c</b>	<i>C</i> <sub>s</sub>		12.7	62.8	351.5	18.1	–				64.7	15.2
<b>1d</b>	<i>C</i> <sub>s</sub>		–27.8	22.1	109.1	–1.6	+12.4	–26.7	–20.7	0.516	65.0	4.0
<b>3b</b>	<i>C</i> <sub>2v</sub>	–	18.4	57.6	363.9						51.4	16.7
<b>4a</b>	<i>C</i> <sub>2v</sub>	–	131.8	62.4	363.9						45.1	17.1
<b>4c</b>	<i>C</i> <sub>s</sub>	–	123.4	26.5	37.0		+18.7	–1.6	+1.7	0.902	57.4	3.0
<b>5a<sup>c</sup></b>	<i>C</i> <sub>1</sub>	CH <sub>2</sub>	77.0 86.7	257.4 24.8	31.7	64.4					64.2	1.0
<b>6a</b>	<i>C</i> <sub>s</sub>	BH	22.7	14.1	–10.7		+27.0	+10.8	+5.0	1.023	73.1	–0.5
<b>6c</b>	<i>C</i> <sub>s</sub>		14.2	60.8	346.0		–				54.6	16.0
<b>6d</b>	<i>C</i> <sub>s</sub>		–34.0	12.9	111.1		+12.8	–28.5	–18.4	0.503	66.3	4.1
<b>7a, ax</b>	<i>C</i> <sub>s</sub>	NH	3.5	21.6	19.7		+22.5	+2.7	+2.0	0.952	78.3	1.6
<b>7c, eq</b>	<i>C</i> <sub>s</sub>		28.0	62.3	352.5		–				61.0	15.8
<b>7d, eq</b>	<i>C</i> <sub>s</sub>		–12.5	27.5	143.5		+10.8	–37.6	–29.5	0.461	71.3	4.3
<b>8a</b>	<i>C</i> <sub>s</sub>	O	20.6	19.6	16.8		+22.2	+3.9	–0.8	0.990	73.5	1.6
<b>8c</b>	<i>C</i> <sub>s</sub>		49.0	61.4	355.0						59.6	15.3
<b>8d</b>	<i>C</i> <sub>s</sub>		9.5	32.3	162.6		+9.3	–42.7	–34.7	0.408	66.6	4.4
<b>9a<sup>c</sup></b>	<i>C</i> <sub>1</sub>	CH <sub>2</sub> CH <sub>2</sub>	–11.4 –11.2	34.5 34.7	203.1	26.3 26.8	+6.9	–58.0	–42.6	0.236	74.8	8.3
<b>9c<sup>c</sup></b>	<i>C</i> <sub>1</sub>		31.6 35.3	66.4 66.1	334.4	23.7 24.1					71.6	15.6
<b>9d</b>	<i>C</i> <sub>s</sub>		–0.8	42.6	277.8	30.4	+2.9	–83.9	–58.5	0.128	69.4	12.8
<b>10a<sup>c</sup></b>	<i>C</i> <sub>1</sub>	CH <sub>2</sub> CH <sub>2</sub>	73.0 79.1	67.9 43.3	–22.1	31.2 28.0					85.6	–1.2

<sup>a</sup> <sup>13</sup>C shifts in ppm relative to TMS, magnetic susceptibility in 10<sup>–6</sup> cm<sup>3</sup> mol<sup>–1</sup>. *P* defines the position of the two-electron, three-center (2e3c) localized MO (LMO). See eq 2. Abbreviations ax and eq denote axial and equatorial positions of the NH bond. <sup>b</sup> Experimental values from ref 21. <sup>c</sup> Second line gives shifts for C5, C4, and C7.

Table 4. Mulliken Charges Calculated from MP2/6-31G(d) Response Density<sup>a</sup>

compd	sym	X	atomic charges				group charges			
			C1	C2	C3	X6	C1	C2	C3	X6
<b>1a</b>	<i>C</i> <sub>3v</sub>	CH <sub>2</sub>	–0.155	–0.343	–0.155	–0.343	0.140	0.192	0.140	0.192
<b>1b</b>	<i>C</i> <sub>s</sub>		–0.191	–0.427	0.127	–0.350	0.071	0.148	0.439	0.121
<b>1c</b>	<i>C</i> <sub>s</sub>		–0.180	–0.440	0.102	–0.368	0.074	0.176	0.416	0.082
<b>1d</b>	<i>C</i> <sub>s</sub>		–0.243	–0.355	–0.016	–0.342	0.056	0.196	0.304	0.193
<b>3a</b>	<i>C</i> <sub>2v</sub>		–0.347	–0.468	0.132		0.126	0.152	0.442	
<b>3b</b>	<i>C</i> <sub>2</sub>		–0.344	–0.435	0.100		0.129	0.162	0.417	
<b>4a</b>	<i>C</i> <sub>2v</sub>		–0.123	–0.495	0.112		0.135	0.149	0.432	
<b>4c</b>	<i>C</i> <sub>s</sub>		–0.074	–0.378	–0.120		0.221	0.180	0.197	
<b>5a</b>	<i>C</i> <sub>1</sub>		–0.377	0.077	–0.443	–0.300	–0.078	0.390	0.090	0.261
<b>6a</b>	<i>C</i> <sub>s</sub>	BH	–0.290	–0.343	–0.176	0.348	0.005	0.199	0.120	0.471
<b>6b</b>	<i>C</i> <sub>s</sub>		–0.334	–0.442	0.130	0.315	–0.067	0.135	0.445	0.418
<b>6c</b>	<i>C</i> <sub>s</sub>		–0.321	–0.451	0.100	0.282	–0.065	0.170	0.416	0.375
<b>7a, ax</b>	<i>C</i> <sub>s</sub>	NH	–0.050	–0.357	–0.139	–0.449	0.254	0.190	0.162	–0.051
<b>7b, eq</b>	<i>C</i> <sub>s</sub>		–0.102	–0.407	0.117	–0.521	0.169	0.182	0.429	–0.129
<b>7c, eq</b>	<i>C</i> <sub>s</sub>		–0.088	–0.411	0.116	–0.560	0.172	0.197	0.432	–0.172
<b>7d, eq</b>	<i>C</i> <sub>s</sub>		–0.120	–0.350	0.002	–0.546	0.176	0.224	0.326	–0.127
<b>8a</b>	<i>C</i> <sub>s</sub>	O	0.077	–0.357	–0.158	–0.328	0.378	0.211	0.149	–0.328
<b>8b</b>	<i>C</i> <sub>s</sub>		0.014	–0.427	0.107	–0.366	0.297	0.173	0.423	–0.366
<b>8c</b>	<i>C</i> <sub>s</sub>		0.028	–0.450	0.130	–0.415	0.299	0.180	0.454	–0.415
<b>8d</b>	<i>C</i> <sub>s</sub>		0.023	–0.368	0.003	–0.427	0.328	0.219	0.332	–0.427
<b>9a</b>	<i>C</i> <sub>1</sub>	CH <sub>2</sub> CH <sub>2</sub>	–0.270	–0.358	0.036	–0.320	0.001	0.182	0.352	0.140
<b>9c</b>	<i>C</i> <sub>1</sub>		–0.199	–0.460	0.160	–0.341	0.046	0.129	0.488	0.081
<b>9d</b>	<i>C</i> <sub>s</sub>		–0.253	–0.383	0.088	–0.326	0.010	0.160	0.407	0.120
<b>10a</b>	<i>C</i> <sub>1</sub>		–0.089	–0.287	–0.436	–0.379	0.203	0.260	–0.142	0.098

<sup>a</sup> Charges in electron. Abbreviations ax or eq indicate that the NH bond is in an axial or equatorial position.

twist form **4b** (Scheme 2) is not stable and rearranges to **4c**. In **4c**, through-space interactions and HA two-electron delocalization are more important than angle strain, eclipsing strain, or hyperconjugative interactions, and therefore, the cation folds as much as possible to increase orbital overlap. In the planar form **4a**, through-space interactions are largely reduced, and accordingly,

**4a** resembles more a classical cation such as **3** as is indicated by charge distribution (Table 4) and calculated chemical shifts of C<sup>+</sup> (Table 3).

Since cation **4c** seems to be a suitable reference molecule for **1a**, it is interesting to assess its HA stabilization energy and compare it with the corresponding energy for **1a**. In a first approximation, the energy

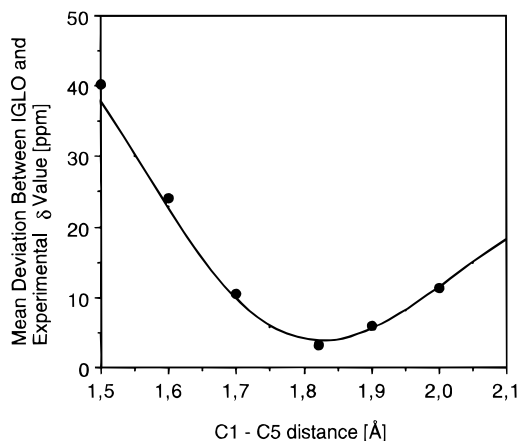


**Figure 2.** Determination of the equilibrium value of distance C1C5 (C1C3, C3C5) by IGLO NMR chemical shift calculations. The minimum of the mean deviation of IGLO  $\delta^{13}\text{C}$  chemical shifts defines the equilibrium value of distance C1C5 (1.82 Å). difference  $E(\mathbf{4a}) - E(\mathbf{4c})$  can be used as an indicator for the degree of HA stabilization of  $\mathbf{4}$ . Schleyer and co-workers<sup>47</sup> report a MP3/6-31G(d)//HF/6-31G(d) energy difference of 13 kcal/mol, which according to our MP4-(SDQ)/6-31G(d)//MP2/6-31G(d) calculations is too large by 7 kcal/mol ( $E(\mathbf{4a}) - E(\mathbf{4c}) = 6$  kcal/mol, Table 2). The corresponding energy difference for  $\mathbf{1a}$  can be obtained by calculating the envelope form  $\mathbf{1e}$  with a folding angle  $\zeta = 180^\circ$  and a planar five-membered ring. Form  $\mathbf{1e}$  is 12.6 kcal/mol (MP4(SDQ)//MP2, Table 2) higher in energy than  $\mathbf{1a}$  and is characterized by a relatively short C1C5 distance (1.522 Å, MP2/6-31G(d), Table 1), i.e., it is close to form  $\mathbf{1d}$  with a fixed C1C5 distance. Obviously, through-space interactions are more effective for  $\mathbf{1a}$  than for  $\mathbf{4c}$  although in the later case the interacting orbitals are closer in energy.

Both  $\mathbf{1d}$  and  $\mathbf{1e}$  are not ideal reference forms since residual through-space interactions and, therefore, residual HA interactions are still present. Because of a folding angle  $\eta = 110.2^\circ$  (MP2/6-31G(d), Table 1), the symmetric Walsh orbital of the three-membered ring is pointing toward the  $p\pi$  orbital at C3, thus leading to significant overlap. Even in planar  $\mathbf{4a}$ , the parallel aligned  $\pi$  orbitals of double bond and  $\text{C}^+$  atom have a residual overlap of 0.05 although they are 2.33 Å apart. Also, hyperconjugative and strain effects are very different in the forms compared, which altogether leads to the fact that the HA stabilization energies for both  $\mathbf{1}$  and  $\mathbf{4}$  are considerably underestimated by the energy differences  $E(\mathbf{1a}) - E(\mathbf{1e})$  and  $E(\mathbf{4a}) - E(\mathbf{4c})$ , respectively.

**Geometric Requirements for Homoaromatic Electron Delocalization.** The energetic consequences of through-space interactions between the symmetric Walsh orbital  $w_s$  and the empty  $p\pi$  orbital at C3 depend on two factors, namely, orbital overlap and the energy difference of the interacting orbitals. The orbital overlap  $S$  can be estimated using the orbital inclination angles  $\omega_1$  and  $\omega_2$  and the distance  $h$ , which can be derived from the geometrical parameters  $\eta$  and  $\zeta$  and distance C1C3, respectively (Figure 1). For  $\mathbf{1a}$ , we calculate at the MP2/6-31G(d) level  $\omega_1 = 34.8^\circ$  and  $\omega_2 = 24.9^\circ$ , which indicates that the overlap is somewhat closer to pure  $\sigma$ - than pure  $\pi$ -overlap. At a C1C3 distance of 1.82 Å, it is 0.25, which is comparable to  $p\pi(\text{C}) - p\pi(\text{C})$  overlap in a conjugated hydrocarbon.

Through-space orbital interactions lead to delocalization of the two electrons of bond C1C5 in the triangle

C1C3C5, which is nicely reflected by calculated MOs, charges, and chemical shifts. For example, upon localization of canonical MOs by Boys localization 6 core orbitals, 15 bond orbitals corresponding to 6 CC and 9 CH bonds, and one two-electron, three-center (2e3c) orbital result. The 2e3c-LMO is located 0.124 Å above the center of the triangle C1C3C5. If the distance C1C5 is decreased to 1.50 Å as in  $\mathbf{1d}$ , the energy of the symmetric Walsh orbital will be lowered and the interactions with the  $p\pi(\text{C3})$  orbital will be reduced since these depend on the orbital energy difference  $\epsilon(w_s) - \epsilon(p\pi(\text{C3}))$ . HA interactions are weakened, and the stability of the cation is decreased. This is reflected by a distortion of the 2e3c-LMO, which is no longer positioned above the center of the triangle C1C3C5 but shifted toward the bond C1C5, in line with the increasing dominance of orbital  $w_s$  and the smooth change from a 2e3c- to a 2e2c-CC bond orbital. This perturbation of the 2e3c orbital and, thereby, of the HA of  $\mathbf{1a}$  can be described by a geometrical parameter  $P$ , which we have defined in the following way:

$$P = (h - b \cos \beta)/(h - R) \quad (1)$$

where  $R$  is the radius of the circumscribed circle of the triangle C1C3C5,  $h$  its altitude, and  $b \cos \beta$  the projection of the position vector  $b$  for the centroid of charge onto the altitude  $h$  as shown in Figure 1b. According to eq 1,  $P$  should be zero for a classical 2e2c orbital localized in the bond C1C5 ( $h = b \cos \beta$ ), 1 for the homoaromatic case ( $b \cos \beta = R$ ), and 3 for the hypothetical case that the electron pair is localized at C3 rather than in the bond C1C5.

For  $\mathbf{1a}$ ,  $P$  is exactly 1, indicating the existence of a perfect HA system. For  $\mathbf{1d}$ , the  $P$  value drops to 0.5, in line with reduced through-space interactions and smaller HA electron delocalization. But despite this reduction,  $P$  indicates that  $\mathbf{1d}$  still benefits from HA interactions and, therefore, it is far from resembling a classical carbocation. There exists a 2e3c orbital in  $\mathbf{1d}$  that causes considerable delocalization of positive charge.

A more suitable reference system for  $\mathbf{1a}$  should be the corresponding boat form  $\mathbf{1c}$ . In such a form, the  $w_s$  and the  $p\pi(\text{C3})$  orbitals are oriented in different directions, thus avoiding overlap and through-space interactions. Form  $\mathbf{1c}$  should represent a classical bicyclo[3.1.0]hex-3-yl cation that can be used as a reference for the nonclassical cation  $\mathbf{1a}$ . Actually, conformation  $\mathbf{1c}$  is better described as an envelope rather than a boat form since its folding angle  $\zeta$  ( $189^\circ$ , MP2/6-31G(d), Table 1) is close to  $180^\circ$ . At MP4(SDQ)/6-31G(d), form  $\mathbf{1c}$  is 17.4 kcal/mol (ZPE corrected 16.8 kcal/mol) less stable than the HA form  $\mathbf{1a}$ . The corresponding energy differences at the HF level (10.8 kcal/mol, Table 2) and at the MP2 level (23.9 kcal/mol) reflect the tendencies of these methods either to overestimate or to underestimate the stability of classical carbocations such as  $\mathbf{1c}$ . This is the reason why all energies reported in the present work have been checked at the MP4(SDQ) level of theory since previous investigations have revealed that at this level of theory a reasonable description of nonclassical cations is obtained. We conclude that the HA stabilization energy of  $\mathbf{1a}$  is at least 17 kcal/mol. Hyperconjugative effects (stabilization of  $\mathbf{1c}$ ) and strain effects do not allow for a more accurate value of the HA stabilization energy.

In Figure 3, the ring-puckering potential of cation  $\mathbf{1}$  calculated at the MP4(SDQ)/6-31G(d) level of theory is

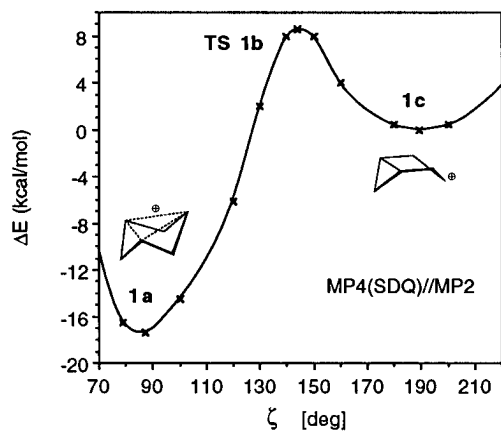


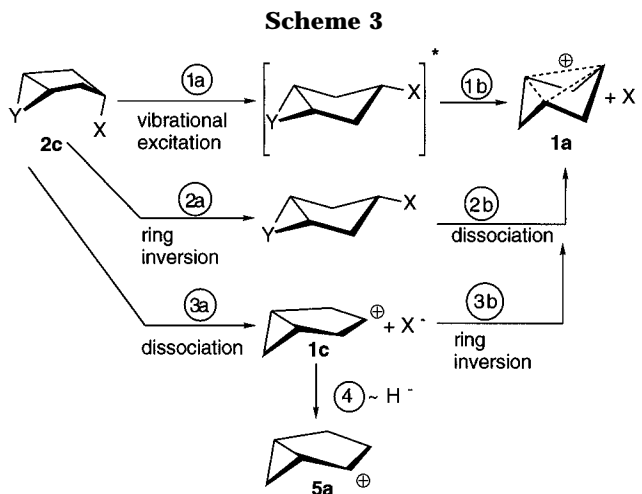
**Figure 3.** Puckering potential of the six-membered ring of cation **1** as a function of the folding angle  $\zeta$  (MP4(SDQ)//MP2/6-31G(d) calculations).

shown as a function of the folding angle  $\zeta$ . The envelope form **1c** is separated by a barrier of 8.6 kcal/mol from the chair form **1a**, which means that if **1c** is formed at room temperature it is likely that cation **1** inverts to the more stable HA form **1a**. However, an equilibrium between **1a** and **1c** is not possible at room temperature since the barrier for the reverse process is 26 kcal/mol (MP4(SDQ)//MP2, Table 2). The TS form **1b** is located at  $\zeta = 144^\circ$  (MP2/6-31G(d), Table 1), i.e., the chair form is already developed, but HA interactions are relatively weak as is reflected by a C1C5 distance of 1.545 Å and a C1C3 distance of 2.278 Å. TS **1b** is destabilized by increased eclipsing and bond angle strain and, in addition, does not benefit from hyperconjugation in the same way as the envelope form **1c**.

#### 4. Formation of Trishomocyclopropenylum Cations

Far-infrared, Raman, microwave, and electron diffraction studies have shown that bicyclo[3.1.0]hexane (**2**) has a ring-puckering potential function with a single minimum occupied by a boat conformation (**2c**).<sup>28–31</sup> The boat conformation has been confirmed by various ab initio investigations,<sup>27,49,50</sup> but in two of these studies also a local minimum for the chair form **2a** (Scheme 2) has been found. Siam and co-workers<sup>49</sup> calculate **2a** to be 3 kcal/mol higher in energy than **2c** at the HF/4-21G level of theory. Okazaki and co-workers<sup>50</sup> have confirmed this prediction by HF/3-21G geometry optimizations and HF/6-31G(d)//HF/3-21G single-point calculations. Further indication for a chair conformation is given by MM2 investigations of Cooper and Laane<sup>51</sup> who obtained a local minimum for the chair form in the ring-puckering potential. On the other hand, Mjöberg and Almlöf<sup>27</sup> found in their HF/DZ investigation of the ring-puckering potential of **2** only the boat minimum and a shoulder at the position of the chair form in agreement with far-infrared and Raman studies.<sup>28,30</sup> However, these authors did not optimize the geometry of **2** for various degrees of puckering, and therefore, their results are questionable.

In case of cis substituents at C3, the chair form **2a** has been experimentally observed. For example, Traetteberg



and co-workers<sup>33</sup> found in an electron diffraction study of 3-chlorobicyclo[3.1.0]hexane that the cis isomer exists in a mixture of 80% boat and 20% chair conformation while the trans isomer exclusively exists in the boat form. However, in NMR studies of a large number of substituted bicyclo[3.1.0]hexanes, Rees and Whittaker<sup>32</sup> exclusively found the boat form by analysis of vicinal coupling constants.

Depending on whether a chair form exists for derivatives of **2**, various mechanisms are possible for the solvolysis process (Scheme 3). In the case of a single minimum potential function, heterolytic dissociation of the bond C3X occurs in a vibrationally excited state associated with a large amplitude inversion motion of the ring (path 1a–1b, Scheme 3). Such a process has been suggested by Mjöberg and co-workers.<sup>52</sup> Alternatively, there could be a conformational equilibrium between boat and chair forms which precedes the actual dissociation step as was originally assumed by Winstein and co-workers (path 2a–2b, Scheme 3).<sup>20</sup> Finally, there could be heterolytic dissociation of the CX bond already in the boat form, thus leading to a boat (envelope) form of the cation **1** (**1c**, Scheme 3), which could rearrange via TS **1b** to the HA cation **1a** (path 3a–3b, Scheme 3). In this case, however, anchimeric assistance cannot be provided by the cyclopropane ring. Also, it would be likely in this case that the nonstabilized cation **1c** would rearrange to the more stable [3.1.0]hex-2-yl cation (**5**, Scheme 3) by a hydride shift which may not require much energy.<sup>25</sup>

Since the existence or nonexistence of a chair form of **2** and its derivatives is of relevance for the mechanism of the solvolysis reaction, we have tried to resolve contradictions between experimental and theoretical descriptions of the ring-puckering potential of **2** by calculating boat and chair forms of **2** at more accurate levels of theory than was previously done.<sup>27,49,50</sup> In agreement with previous investigations, we find that a somewhat flattened boat **2c** ( $\eta = 112.0$  and  $\zeta - 180 = 28.8^\circ$  at MP2/6-31G(d), expt values 117, 38<sup>29</sup> and 109, 25<sup>31</sup>, Table 1) corresponds to the equilibrium conformation of **2**. The calculated conformation can be considered the result of mixing to an ideal boat form (90.8%) 9.2% of a chair form so that the five-membered ring part becomes flatter.<sup>53–55</sup>

(49) Siam, K.; Ewbank, J. D.; Schäfer, L.; Alsenoy, C. v. *J. Mol. Struct. (Theochem)* **1987**, 150, 121.

(50) Okazaki, R.; Niwa, J.; Kato, S. *Bull. Chem. Soc. Jpn.* **1988**, 61, 1619.

(51) Rosas, R. L.; Cooper, C.; Laane, J. *J. Phys. Chem.* **1990**, 94, 1830.

(52) Mjöberg, P. J.; Norin, T.; Weber, M. *Acta. Chem. Scand.* **1975**, Ser. B, 29, 1039.

(53) This can be calculated from the puckering coordinates of the six-membered ring.<sup>54</sup>

(54) Cremer, D.; Pople, J. A. *J. Am. Chem. Soc.* **1975**, 97, 1354.

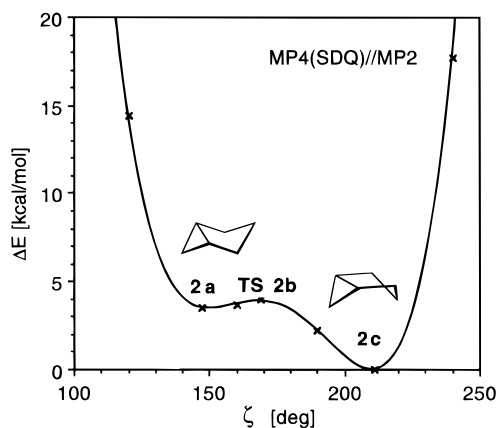


**Figure 4.** Puckering potential of the six-membered ring of bicyclo[3.1.0]hexane (**2**) as a function of the folding angle  $\zeta$  (MP4(SDQ)//MP2/6-31G(d) calculations).

Both at the HF/6-31G(d) and MP2/6-31G(d) level of theory, a local minimum for the chair form is obtained, which is 3.4 and 3.7 kcal/mol, respectively, higher in energy than the global minimum occupied by the boat form. MP2/6-31G(d) folding angles  $\eta$  and  $\zeta$  for the chair are 111.6 and 147.4° (Table 1), which again reveal considerable flattening of the five-membered ring part. According to calculated puckering coordinates,<sup>54</sup> form **2a** is best viewed as a chair form (63%) that is considerably flattened by an admixture of 37% of the boat form.<sup>53–55</sup>

TS **2b** of the boat–chair ring inversion is located close to the chair form and is just 0.5 kcal/mol (MP4(SDQ)/6-31G(d)//MP2/6-31G(d); 0.2, HF/6-31G(d); 0.8, MP2/6-31G(d), Table 2) above the energy of **2a**. If zero-point energy corrections calculated at the HF level are added, the energy difference between **2a** and TS **2b** decreases by 0.1 to 0.4 kcal/mol at MP4(SDQ)//MP2/6-31G(d), which means that at normal temperatures ( $RT = 0.6$  kcal/mol) there practically exists no second minimum. The ring-puckering potential shown in Figure 4 is best described as a single-minimum potential with a distinct shoulder at the position of the chair form. This fully explains the seemingly contradictory descriptions of the ring-puckering potential of **2** given by far infrared and Raman spectroscopy on the one hand (single-minimum potential<sup>28,30</sup>) and ab initio calculations on the other hand (asymmetric double-minimum potential<sup>49,50</sup>).

One could argue that the potential function shown in Figure 4 is of little relevance for the actual conformation of 3-substituted bicyclo[3.1.0]hexanes since a cis substituent in the flagpole position of the boat leads to considerable steric repulsion and, therefore, to a preference of the chair conformation. However, because of the flattening of the boat form steric repulsion between a cis substituent at C3 and the H atom at C6 is of minor consequence. The relative stability of boat and chair form is dominated by the eclipsing strain involving HC1, HC2, and HC3. Since this will always be smaller for the boat form, one can expect that also cis-substituted **2** has a potential function similar to the one shown in Figure 4, where the local minimum for the chair form may be more pronounced as is suggested by the electron diffraction results of Traetteberg and co-workers.<sup>33</sup>

The activation enthalpy for the solvolysis of 3-bicyclo[3.1.0]hexyl tosylate has been measured to be 24 kcal/mol.<sup>19</sup> From the discussion given above, we conclude that part of this energy is used for the vibrational excitation of the boat form (or for the boat–chair inversion) and the rest for the heterolytic breakage of the CO bond, which can be supported by a polar solvent. At the beginning of CO bond dissociation, the folding angle  $\zeta$  will be about 150° (see **2a**, Table 1). As can be seen from the puckering potential of **1a** shown in Figure 3, a folding angle of 150° corresponds to a conformer that is located on the boat side of the ring inversion process. Geometry relaxation of this conformer would lead to the envelope form **1c** rather than the HA chair form **1a**. The envelope form **1c**, in turn, will rapidly rearrange by a hydride shift to cation **5**. Migration of the trans H at C2 (with regard to the cyclopropyl group) requires just 1.1 kcal/mol (MP4(SDQ)//MP2/6-31G(d)+ZPE/HF/6-31G(d), Table 2) while migration of the cis H has a somewhat higher barrier. Cation **5** is 20.5 kcal/mol (MP4(SDQ)/6-31G(d)//MP2/6-31G(d), Table 2) more stable than the envelope form **1c** and 3.1 kcal/mol more stable than the HA form **1a** because of the energetically favorable cyclopropylcarbinyl cation unit characteristic for **5**. The corresponding MINDO/3 energies of Jørgensen (16.5 and 3.9 kcal/mol)<sup>25</sup> are surprisingly close to these results.

If cation **1c** is formed in the solvolysis process, then the main product will be cation **5** rather than the HA cation **1a**. However, the formation of **1c** is not facilitated by anchimeric assistance of the cyclopropyl group and, therefore, is unlikely to be the dominant process. More likely is that dissociation of the CX bond (X = OTs, Cl, etc.) is accompanied by a decrease of the folding angle  $\zeta$  as originally anticipated by Winstein.<sup>19,20</sup> The bond C1C5 approaches C3 from the backside and pushes out X<sup>−</sup>. Solvolysis of **2c** probably proceeds via path 1a–1b in Scheme 3. Path 2a–2b may be possible for certain derivatives of **2**, which possess a well-developed chair minimum on the PES. However, paths 3a–3b or 3a–4 will be the exception rather than the rule for heterolytic dissociation of derivatives of **2**. These predictions are based on gas phase energies, but in view of the well-known correspondence of kinetic and thermodynamic parameters for the rearrangements of isomeric carbocations in gas phase and solution phases,<sup>4</sup> they should be equally valid for the actual solvolysis reactions.

### 5. Remote Perturbation of Trishomoaromaticity by a Heteroatom

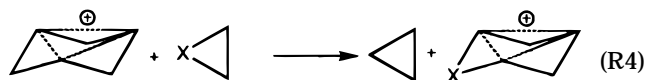
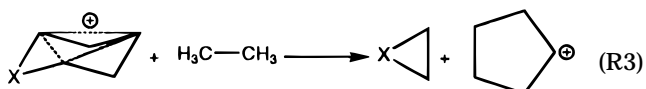
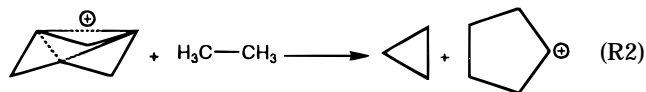
The effect of a heteroatom on HA interactions in **1a** can be investigated by replacing the CH<sub>2</sub> group of the cyclopropyl ring by X = BH (**6**), NH (**7**), O (**8**), etc. This leads to changes in the symmetric Walsh  $w_s$  orbital both with regard to orbital energy and orbital amplitude, which in turn affect through-space interactions with the  $p\pi(C3)$  orbital according to PMO formula (2).

$$\Delta E(w_s, p\pi) \propto \frac{S^2(w_s, p\pi)}{|\epsilon(w_s) - \epsilon(p\pi)|} \quad (2)$$

An electropositive (electronegative) atom X replacing C6 should increase (decrease) through-space interactions and HA electron delocalization. Changes in energy caused by X can be determined with the help of the formal reactions 2, 3, and 4. Reaction energies  $\Delta_R E$  of (2) and (3), respectively, cover the HA stabilization

(55) Cremer, D.; Szabo, K. J. In *Methods in Stereochemical Analysis, Vol. Conformational Behavior of Six-Membered Rings*; Juaristi, E., Ed.; VCH Publishers: New York, 1995.

(56) Radom, L.; Poppinga, D.; Haddon, R. C. *Carbocation Ions*; Olah, G. A., Schleyer, P. v. R., Eds.; Wiley: New York, 1976; Vol. V, p 2303.



energy, changes in strain, and hyperconjugative and inductive effects and, therefore, are not suitable for a reliable determination of the HA stabilization energy itself (vide infra). However, the reaction energy of (4), which corresponds to the difference  $\Delta_{\text{R}}E(2) - \Delta_{\text{R}}E(3)$ , should provide an appropriate measure for the change in HA stabilization energies upon incorporation of X into **1a** since changes in strain, hyperconjugation, and inductive effects should be similar for reactions 2 and 3. Therefore, calculated MP4(SDQ) values of reaction 4 for X = CH<sub>2</sub>, BH, NH, and O are listed in Table 5.

**6-Borabicyclo[3.1.0]hex-3-yl Cation (6).** Replacement of the cyclopropyl ring by a borirane ring raises  $\epsilon(w_s)$  and, thereby, decreases the energy difference  $\epsilon(w_s) - \epsilon(p\pi)$ . Accordingly, through-space interactions should be enhanced by X = BH, which is fully confirmed by the calculated properties of **6a**:

(a) For **6a**, there is a larger charge transfer from the three-membered ring to C3 than for any of the other cations calculated (Table 4). As a consequence, the nucleus of C3 is more shielded than in cation **1a**. This is reflected by the calculated  $\delta^{13}\text{C}3$  value of  $-15.7$  ppm (Table 3), which is more than 16 ppm shifted to higher field. The corresponding value for C1 (C5) (23.6 ppm) is shifted by more than 20 ppm to lower field, suggesting that the nucleus of C1 (C5) is deshielded compared to **1a**.

(b) Because of the increased charge transfer, the C1C5 bond is weaker than in cation **1a**. We calculate a MP2/6-31G(d) value of 1.995 Å (Table 1). At the same time, the folding angle  $\zeta$  is decreased to 82.6° (**1a**,  $\zeta = 87.1$ , Table 1) to guarantee a C1C3 distance (1.851 Å, Table 1) and orbital overlap comparable to that in cation **1a**. It is interesting to note that a reduction of  $\zeta$  implies an increase of folding angle  $\eta$  (from 117.4, **1a**, to 127.7°, **6a**) to have symmetric Walsh orbital and  $p\pi(\text{C}3)$  orbital directed in such a way that orbital overlap between them is most effective.

The consequences of enhanced through-space interactions are increased tris-HA and stability of **6a** as is nicely reflected by the energies of reactions 2, 3, and 4, which are 22.1, 24.5, and  $-2.4$  kcal/mol, respectively (MP4(SDQ)//MP2/6-31G(d), Table 5). Also, the energy difference between **6a** and its envelope form **6c** (23.7 kcal/mol, ZPE corrected 21.7 kcal/mol, Table 2) is 6 kcal/mol larger than the corresponding energy difference for cation **1** while the barrier to chair–envelope interconversion (31.2 kcal/mol, ZPE corrected 29.3 kcal/mol, form **6b**, Table 2) is about 5 kcal/mol larger.

Probably, **6** exists in the form of a B–H–B bridged dimer rather than a monomer. MP2/6-31G(d) calculations for boracyclopropane and its dimer indicate that the energy of the symmetric Walsh orbital increases slightly from  $-0.40369$  to  $-0.39733$  hartree due to dimerization,

**Table 5. Stabilization Energies Calculated at the MP4(SDQ)//MP2/6-31G(d) Level of Theory<sup>a</sup>**

compd	X	$E(c) - E(a)$	$\Delta_{\text{R}}E(3)$	$\Delta_{\text{R}}E(4)$
<b>1</b>	CH <sub>2</sub>	17.4	22.1	0
<b>6</b>	BH	23.7	24.5	$-2.4$
<b>7</b>	NH	9.5	17.5	4.6
<b>8</b>	O	4.3	6.9	15.2
<b>9</b>	CH <sub>2</sub> CH <sub>2</sub>		$-1.8$	20.3
<b>4</b>		6.0 <sup>b</sup>		

<sup>a</sup> All energies in kcal/mol.  $E(c) - E(a)$  denotes the energy difference between envelop and chair forms,  $\Delta_{\text{R}}E(2)$  and  $\Delta_{\text{R}}E(4)$  the energies of reactions 2 and 4. <sup>b</sup> Energy difference between **4a** and **4c**.

suggesting that the symmetric Walsh orbital and  $p\pi(\text{C}3)$  orbital interact more effectively in the dimer of **6** than its monomer, thus enhancing the trend discussed above. The dimerization energy for boracyclopropane is  $-33.6$  kcal/mol at MP2/6-31G(d) (fully optimized geometries). A similar stabilization can be expected for the dimer of **6**, which makes it an interesting target of synthesis.

**6-Azabicyclo[3.1.0]hex-3-yl Cation (7).** The influence of a N atom on the properties of the symmetric Walsh orbital in a three-membered ring is 2-fold. First, the electron-withdrawing nature of N leads to a buildup of positive charges at the C atoms of aziridine, followed by orbital contraction and lowering of the  $w_s$  orbital energy. Second, the lone pair orbital of N can mix with the  $w_s$  orbital provided bonds at the N atom are pyramidally arranged. As a consequence of this mixing, there are two orbitals that can interact with the  $p\pi(\text{C}3)$  orbital. The high-lying orbital, which is predominantly a lone pair orbital, has rather small amplitudes at the C atoms and, thereby, rather small overlap with the  $p\pi(\text{C}3)$  orbital, while the other orbital is relatively low in energy, thus leading to reduced interactions according to eq 2. Despite the fact that the  $p\pi(\text{C}3)$  orbital can interact with two three-membered ring orbitals in **7**, through-space interactions in **7a** are considerably smaller compared to those in **1a** as is reflected by the following properties.

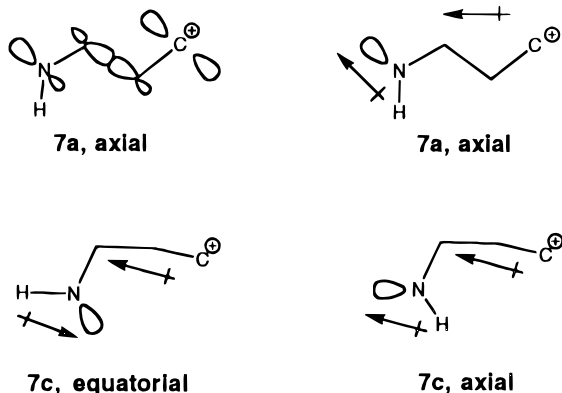
(a) Because of electron withdrawal by the N atom, charge transfer from C1 and C5 to C3 is smaller than in either **1a** or **5a** (Table 4). IGLO  $\delta^{13}\text{C}$  values (C3 19.7; C1 3.5 ppm, Table 3) are in line with the calculated charge distribution.

(b) The MP2/6-31G(d) distance C1C5 (1.74 Å, Table 1) is 0.08 Å smaller, while the C1C3 distance (1.86 Å) is 0.03 Å longer than in **1a**. The folding angle  $\zeta$  opens up to 92°.

(c) The chair–envelope energy difference is just 9.5 kcal/mol (ZPE corrected 8.2 kcal/mol) and the corresponding barrier just 21.2 kcal/mol at the MP4(SDQ)//MP2 level (ZPE corrected 19.4 kcal/mol). The energy of the formal reaction 3 is 17.5 kcal/mol (Table 5), i.e., the HA stabilization energy of **7a** is 4.6 kcal/mol smaller (reaction 4, Table 5) than in the case of **1a**.

In **7a**, the axial NH bond is 3.3 kcal/mol (MP4(SDQ)//MP2/6-31G(d), Table 2) more stable than the equatorial NH bond. This is caused partially by NH,CH bond eclipsing and partially by favorable through-bond interactions that involve the lone pair orbital at N, the C1C2 (C5C4)  $\sigma$  orbital, and the  $p\pi(\text{C}3)$  orbital. If the chair form **7a** rearranges to the envelope form **7c**, another effect will emerge, namely, stabilizing electrostatic interactions between an axially oriented electron lone pair and the positive charge at C3. Envelope form **7c** with an equatorially positioned NH bond gains almost 9 kcal/mol (HF/

6-31G(d), Table 2) with regard to the corresponding axial conformation.



Already, TS **7b** benefits from these interactions and, accordingly, prefers the NH bond in the equatorial rather than the axial position ( $\Delta E = 1.8$  kcal/mol at HF/6-31G(d), Table 2). This means that the chair–envelope inversion is coupled with an inversion at the N atom, which in the case of **7a** requires an activation energy of 14.2 kcal/mol (MP4(SDQ)//MP2/6-31G(d), 12.7 kcal/mol ZPE corrected, Table 2). Hence, inversion at N can precede ring inversion since the energy barrier for the later process is 7 kcal/mol higher (21.2 kcal/mol, ZPE corrected 19.4 kcal/mol, Table 2).

**6-Oxabicyclo[3.1.0]hex-3-yl Cation (8).** Because of the electronegativity of the O atom, the Walsh orbitals of oxirane are lower in energy than those of either cyclopropane or aziridine. As a consequence, the oxirane  $w_s$  orbital is less suitable for through-space interactions with the  $p\pi(C3)$  orbital, but the reduction in orbital interactions relative to aziridine is not so dramatic as is reflected by the calculated properties of **8a**.

(a) Charge transfer from C1 and C5 to C3 is similarly small as in the case of **7a** (Table 4). The IGLO  $\delta^{13}\text{C}$  value for C3 (**8a**) is 16.8 ppm and comparable to that of **7a**. However,  $\delta^{13}\text{C}$  of C1 (20.6 ppm, Table 3) is shifted somewhat to lower field because of the inductive effect of O.

(b) The distance C1C5 (1.706 Å, Table 1) is shorter than that for **1a**, **6a**, or **7a**. The same is true with regard to the distance C1C3, which is surprising in view of the reduced through-space interactions in **8a**.

(c) The energy difference between **8a** and the envelope form **8c** is just 4.3 kcal/mol (ZPE corrected 2.7 kcal/mol) while the TS for the chair–envelope interconversion is 12.5 kcal/mol (MP4(SDQ)/6-31G(d), ZPE corrected 10.8 kcal/mol, Table 2). The MP4(SDQ)/6-31G(d) energy of reaction 3 is 6.9 kcal/mol, which is 15.2 kcal/mol smaller than that for **1a** (reaction 4, Table 5).

We conclude that the HA stabilization energy of **8a** is considerably reduced because of the energy lowering of the symmetric Walsh orbital caused by the O atom.

**Bicyclo[3.2.0]hept-3-yl Cation (9).** Homoconjugation and HA in cations such as **1a** are a result of the  $\pi$ -character of the cyclopropane bonds.<sup>57,58</sup> For cyclobutane, the  $\pi$ -character of the CC bonds is negligibly small,<sup>58</sup> and the orbital energy of the highest occupied  $\sigma(\text{CC})$  orbital that has the right symmetry to interact

with the  $p\pi(C3)$  orbital is considerably lower than the symmetric Walsh orbital of cyclopropane and, in addition, aligned along the CC bond axis rather than bent outwardly in the direction of C3. Therefore, cation **9a** should possess, if at all, only weak HA character.

At the HF/6-31G(d) level of theory, there is a minimum energy structure which corresponds to cation **9a**. This no longer possesses  $C_s$  symmetry but has  $C_1$  symmetry because of twisting of the cyclobutane ring and increased staggering of the  $\text{CH}_2$  groups. Its C1C5 (1.647 Å, Table 1) and C1C3 (2.015 Å) distances together with a folding angle  $\zeta$  of 106.9° suggest reduced but not negligible through-space interactions. However, cation **9a** is neither kinetically nor thermodynamically stable. The HF/6-31G(d) barrier to ring inversion is just 0.9 kcal/mol (TS **9b**, Table 2) and the envelope form **9c** generated in the ring inversion process is 8.8 kcal/mol more stable than chair form **9a**.

At the MP2/6-31G(d) level, stationary points corresponding to **9a** or **9b** no longer exist. There is just the minimum for the envelope form **9c** which suggests that the cyclobutane ring, as expected, is not able to provide anchimeric assistance in the solvolysis reaction. If one uses the HF geometry for **9a** and calculates reaction energies (3) and (4) at MP4(SDQ), then a decrease of HA stabilization by 20.3 kcal/mol relative to **1a** results, again suggesting that residual through-space interactions do not lead to important electron delocalization.

## 6. Rearrangement of the Bicyclo[3.2.0]hept-3-yl Cation (9) to a Center-Protonated Spiropentyl Cation (10): A New Target for Synthesis

MP2 optimization of the bicyclic structure **9a** obtained at the HF level leads to the  $C_1$ -symmetrical tricyclo[4.1.0.0<sup>1,3</sup>]heptyl cation **10a** (Scheme 2) that corresponds to an ethano-bridged center-protonated spirocyclopentane with a pentacoordinated pyramidal carbon atom.<sup>59</sup> Formally, one could also speak of a bishomoallyl cation; however, **10a** is characterized by four rather than two stretched CC bonds (see Figure 5). The MP2 C1C5 distance is 2.432 Å (Table 1), and the C1C3, C2C3, C3C4, and C3C5 distances are 1.622, 1.617, 1.568, and 1.653 Å, respectively. Cation **10a** also exists on the HF PES where it is 13.3 kcal/mol lower in energy than **9a** where the latter form is separated from **10a** by a small energy barrier of 0.7 kcal/mol. Since we started to carry out geometry optimizations of **9** under  $C_s$  symmetry constraint we found first the  $C_s$ -symmetrical form **10b**. However, calculation of vibrational frequencies revealed that **10b** is a first-order TS of a conformational process that connects two twisted ring forms **10a** and **10a'** (see Figure 5) and possesses an energy barrier of 2.0 kcal/mol at the MP4(SDQ)//MP2/6-31G(d) level of theory (1.9 kcal/mol with ZPE corrections, Table 2).

The cation **10a** is a new stationary point on the PES of the cation  $\text{C}_7\text{H}_{11}^+$ , which also harbors the norbornyl cation.<sup>59,60</sup> It represents the missing link between the bicyclo[3.2.0]hept-3-yl cation (**9**) and the norbornyl cation (**11**). This can be realized by considering for reasons of simplicity the  $C_s$ -symmetrical form **10b** and increasing its folding angle  $\nu = 39.6^\circ$  (defined as angle C6C7, C1C5, C3) stepwise to about 100°. By this movement, the bonds

(57) Cremer, D.; Kraka, E. *Molecular Structure and Energetics*; Liebman, J. F., Greenberg, Eds.; VCH: Deerfield Beach, FL, 1988; Vol. 7, p 65.

(58) Cremer, D.; Gauss, J. *J. Am. Chem. Soc.* **1986**, *108*, 7467.

(59) Szabo, K. J.; Cremer, D. *J. Org. Chem.* **1995**, *60*, 2257.

(60) Sieber, S.; Schleyer, P. v. R.; Vancik, H.; Mesic, M.; Sunko, D. *E. Angew. Chem., Int. Ed. Engl.* **1993**, *1993*, 1604. Schleyer, P. v. R.; Sieber, S. *Angew. Chem., Int. Ed. Engl.* **1993**, *32*, 1606.

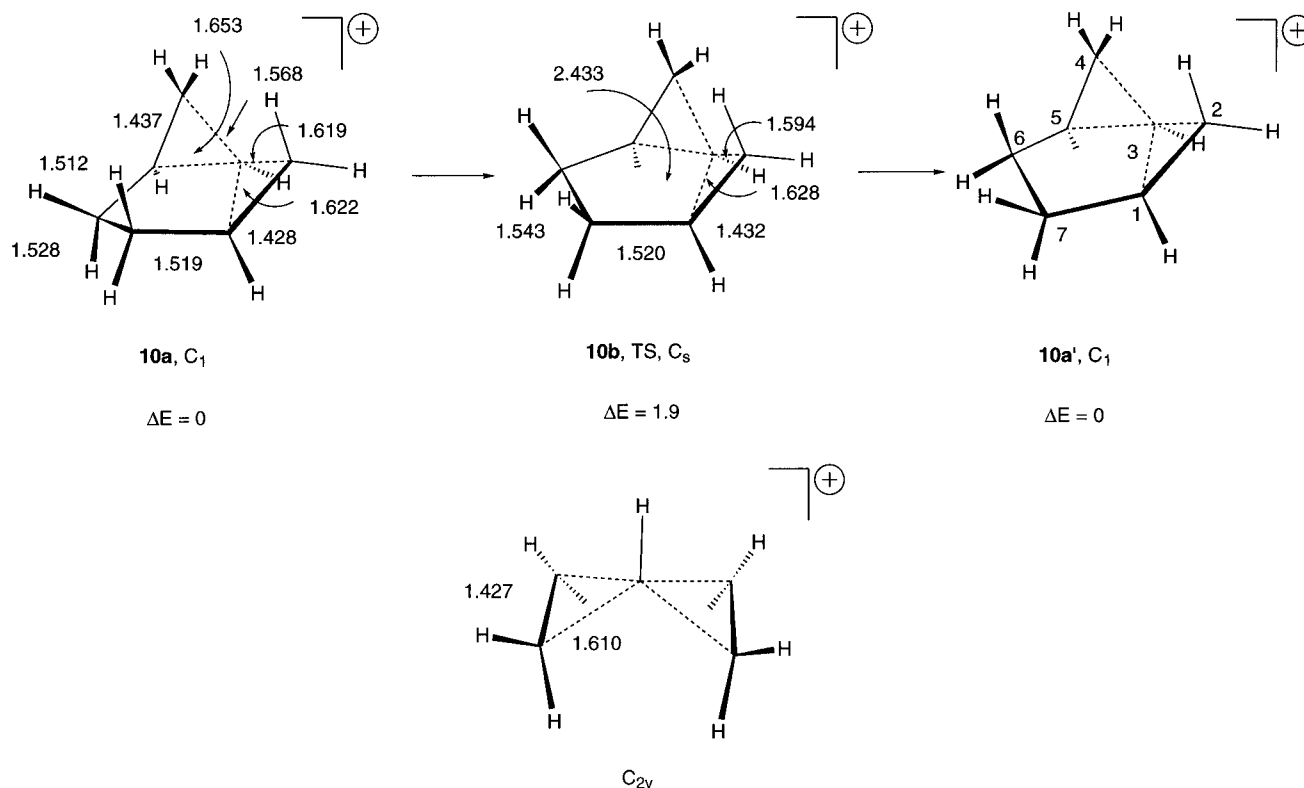


**Figure 5.**  $C_1$ - and  $C_s$ -symmetrical forms **10a** and **10b** of the tricyclo[4.1.0.0<sup>1,3</sup>]heptyl cation. MP2 distances in Å. Energy difference in kcal/mol according to MP4(SDQ)//MP2/6-31G(d)+ZPE calculations.

C2C3 and C3C4 are stretched while the distance C2C4 becomes smaller. At  $\nu = 73.8^\circ$ , the  $C_s$ -symmetrical TS **10c** (C2C4 2.02 Å, C2C3 1.79 Å, Table 1, see also Figure 6) is encountered, which connects **10a** with the  $C_s$ -symmetrical norbornyl cation **11a** ( $\nu = 98.3^\circ$ <sup>60</sup>) and the  $C_1$ -symmetrical cation **11b** (see Figure 6). TS **10c** is 15.9 kcal/mol higher in energy than cation **10a**, 12.9 kcal/mol higher than **11a**, and 16.0 kcal/mol higher than **11b**, i.e., cation **10a** and the bridged norbornyl cation **11b** have identical MP4(SDQ) energies within 0.1 kcal/mol (Table 2). In view of an energy barrier of 16 kcal/mol, it is likely that at low temperatures **10a** does not rearrange via **11a** and **11b** to the more stable 2-norbornyl cation recently described by Sieber and co-workers.<sup>60</sup> So far, cation **10a** has not been observed in connection with experimental studies on norbornyl cations or in the solvolysis reaction of bicyclo[3.2.0]hept-3-yl derivatives, which might have to do with the fact that no one expected such an unusual cation on the  $C_7H_{11}^+$  PES. This work shows that **10a** is an interesting experimental target since it would represent, if synthesized, the first pentacoordinated center-protonated spiropenyl cation ever investigated experimentally.

Figure 6 reveals an interesting reaction mechanism for the rearrangement of **9c** (when formed in a solvolysis reaction of bicyclo[3.2.0]hept-3-yl derivatives) to the norbornyl cation **11b**. The rearrangement proceeds via intermediate **10a** and the three consecutive first-order TSs **10b**, **10c**, and **11a** without any further intermediate. If the bridge-flipping process via the  $C_{2v}$ -symmetrical TS **11c** of the norbornyl cation is also included, then there will be even five consecutive TSs without any intermediate. We have confirmed this sequence of directly following TSs by carrying out intrinsic reaction coordinate calculations. The unusual topology of the potential energy surface in the region of **9** and **11** will become

understandable if one considers that TSs **10b** and **11a** are ("conformational") TSs for stereoisomerization processes between **10a** and **10a'** and **11b** and **11b'**, respectively. Stereoisomerization takes place in both cases along a reaction coordinate vector which is orthogonal to that of the rearrangement **9c**  $\rightarrow$  **11b**.

Three consecutive TSs have recently been found for the degenerate rearrangements of the barbaralyl cation by Cremer and colleagues.<sup>11</sup> These authors have coined the term *double bifurcation mechanism* to describe the mechanistic and kinetic consequences of three consecutive TSs without intermediate. In the present case one would have to speak of a double or triple bifurcation mechanism depending of whether one includes the rearrangement **11a** to **11a'** via TS **11c**. For the hypothetical process leading from **9c** to the rearranged ion **9c'** with atom C3 inserted between C6 and C7, seven consecutive TSs would have to be passed (**10b**, **10c**, **11a**, **11c**, **11a'**, **10c'**, **10b'**) corresponding to four possible reaction path bifurcations and a quadruple bifurcation mechanism. We note that bifurcation mechanisms will be found in symmetrical polycyclic hydrocarbons with several rearrangement possibilities. It seems as if bifurcation mechanisms are indicative of floppy molecules with rapid structural changes at relatively low temperatures.

## 7. Magnetic Properties as a Probe for Homoaromaticity

Direct experimental observation of the tris-HA cation **1a** was so far only possible by NMR spectroscopy.<sup>21-24</sup> Measured <sup>13</sup>C chemical shifts provide the most convincing evidence on the peculiar electronic nature of **1a**. Classical carbocations of the type  $R_2CH^+$  (R = alkyl) possess  $\delta^{13}C$  values above 300 ppm. For example, we calculate for the planar five-membered ring cations **3a** and **4a**

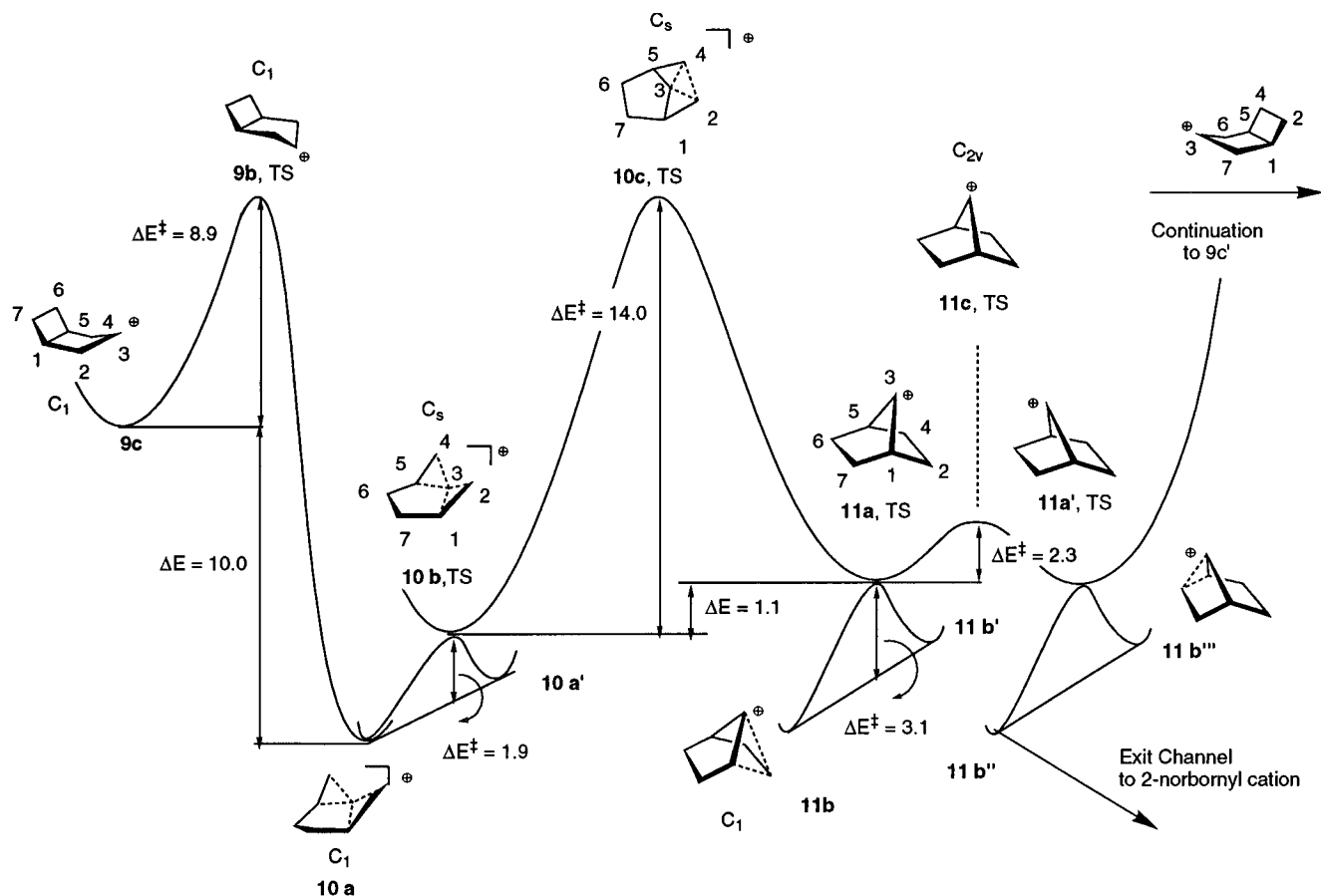


**Figure 6.** Schematic representation of the  $C_7H_{11}^+$  potential energy surface according to MP4(SDQ)//MP2/6-31G(d)+ZPE calculations.

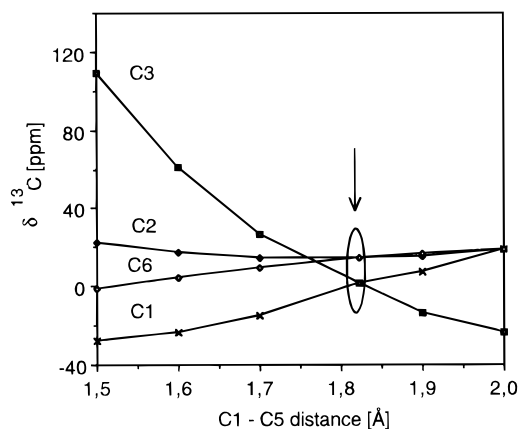


**Figure 7.** IGLO  $\delta^{13}C$  chemical shifts [ppm] of **1** given as a function of the distance C1C5.

IGLO/6-31G(d) values of 364 ppm (Table 3), respectively. For the envelope form **1c**, the calculated  $\delta^{13}C$  value is 352 ppm, suggesting that in this form positive charge is strongly localized at C3. As soon as HA electron delocalization becomes important, negative charge is transferred to C3 and its nucleus is more shielded. This is nicely reflected by Figure 7, which gives IGLO  $^{13}C$  shifts of **1a** as a function of the distance C1C5. For an C1C5 increase from 1.5 to 2 Å, there is a strong change of the shift values of C1 (C5) and C3 while those of C2 (C4) and C6 change only slightly. The  $\delta^{13}C$  value of C1 is shifted 50 ppm to lower field and that of C3, 140 ppm, to higher field. Inspection of Figure 8 shows that changes in chemical shifts are parallel and a result of similar

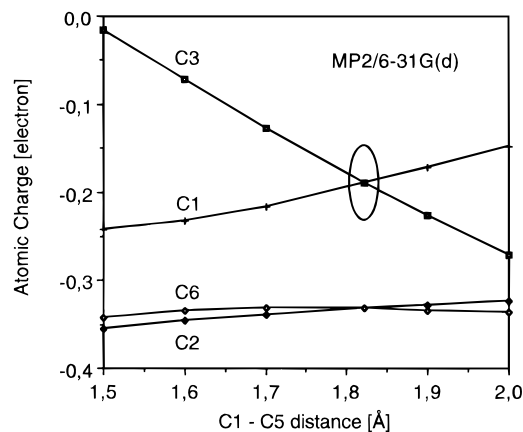


**Figure 8.** Mulliken charges of the C atoms of **1** given as a function of the distance C1C5 (MP2/6-31G(d) calculations).

changes in atomic charges. The nucleus of C3 is more shielded and those of C1 and C5 are deshielded as a result of a lengthening of the distance C1C5 and increased through-space interactions between the symmetric Walsh orbital and the  $p\pi(C3)$  orbital.

The  $\delta^{13}C$  value of C3 seems to be the best indicator for homoconjugation and HA electron delocalization. This can be seen in the case of form **1d**, for which the C1C5 distance is frozen at 1.50 Å. Although one might expect that HA interactions are largely reduced, the shift value of C3 (109 ppm, Table 3) indicates that HA electron delocalization is still significant, leading to a shielding of the C3 nucleus by 260 ppm (cf.  $\delta^{13}C3$  in **1c**). On the other hand, a widening of the folding angle  $\zeta$  as in the

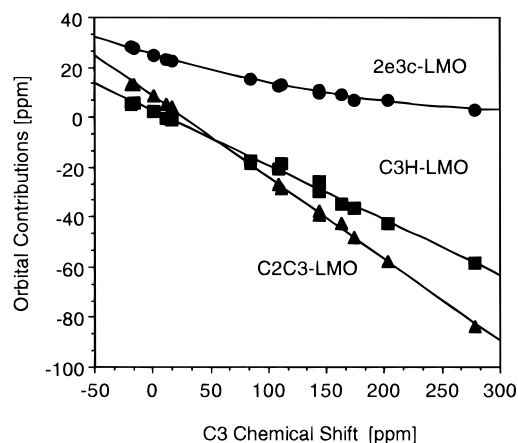


**Figure 9.** IGLO  $\delta^{13}\text{C}$  chemical shifts of various trishomocyclopropenylium cations given as a function of their folding angle  $\zeta$ .

chair-envelope inversion process leads to a very strong reduction of HA interactions as is indicated by  $\delta^{13}\text{C}$  going to 367 ppm for  $\zeta$  going to  $180^\circ$  (Table 3). Therefore, the folding angle  $\zeta$ , if experimentally available, can also be used as an indicator for HA character. It determines the overlap between the symmetric Walsh orbital and the  $p\pi(\text{C}3)$  orbital and, thereby, the degree of HA through-space interactions. This is confirmed by Figure 9, which gives  $\delta^{13}\text{C}$  values as a function of  $\zeta$ . Small folding angles close to  $80^\circ$  are typical of strong HA interactions (**1a**, **6a**) while  $\zeta$  values above  $100^\circ$  are indicative of strongly reduced HA interactions. It is interesting to note that the HA cation **4c** with an IGLO/6-31G(d)  $\delta^{13}\text{C}$  value of 53.1 ppm and a folding angle  $\zeta$  of  $88.7^\circ$  takes on the  $\delta^{13}\text{C}$ - $\zeta$  curve (Figure 9) an intermediate position between the strongly HA cations **1a** and **6a** and cations **1d**, **6d**, **7d**, and **8d** with reduced HA.

Figure 9 suggests that experimentally observed  $\delta^{13}\text{C}$  shift values can be used to obtain direct information on the magnitude of the folding angle  $\zeta$ , the conformation of the cation, and the extent of HA interactions.

Orbital contributions to the absolute shift value of C3,  $\sigma(\text{C}3)$ , constitute a consistent pattern. The largest orbital contribution to  $\sigma(\text{C}3)$  is due to the carbon 1s-AO (200.8 ppm), which is constant for almost all cations investigated in this work<sup>38,44</sup> and, therefore, can be excluded from the discussion. There are four LMO contributions, which dominate the magnitude of  $\sigma(\text{C}3)$ , namely, those of the C2C3 and C3C4 bond orbitals, that of the C3H bond orbital, and, finally, that of the two-electron, three-center (2e3c) LMO found for all HA compounds investigated in this work. For a weakly HA cation such as **9a** (HF geometry),  $\sigma(\text{C}3)$  is dominated by the deshielding LMO contributions associated with bonds C2C3, C3C4, and C3H (Table 3). These deshielding effects are known for classical carbocations to result from paramagnetic currents in the plane of the  $\sigma$ -bonds.<sup>38,44</sup> The magnitude of these effects depends on the availability and energy of the empty  $p\pi$  orbital since it is inversely proportional to  $\sigma$ - $\pi$  excitation energies. In the way, the  $p\pi$  orbital is filled because of HA electron delocalization, the paramagnetic deshielding contributions vanish, and small diamagnetic shielding contributions appear (Table 3 and Figure 10). The contribution by the 2e3c orbital becomes the most shielding one, which can be interpreted in terms of a diamagnetic current above the plane C1C3C5. HA electron delocalization for **1a** and its heteroatomic ana-

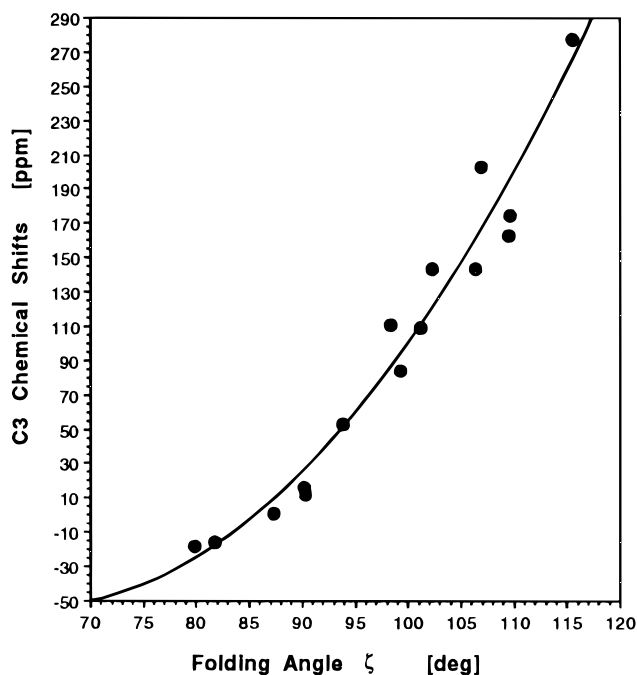


**Figure 10.** Contributions of the 2e3c-, the C2C3-, and the C3H-localized MO (LMO) to the IGLO/6-31G(d)  $^{13}\text{C}$  NMR chemical shift of C3 calculated for various trishomocyclopropenylium cations.

logues **6a**, **7a**, and **8a** is indicated by the lack of strong local paramagnetic ring currents and deshielding bond contributions to  $\sigma(\text{C}3)$  as well as a relatively large shielding contributions of the 2e3c-LMO. Therefore, it is reasonable to use the contribution of the 2e3c-, the C3H-, or the C2C3 (C3C4)-LMO to  $\sigma(\text{C}3)$  as a measure for the HA character of tris-HA compounds (Figure 10).

In view of the role of the 2e3c orbital for the HA character of cation **1a**, it makes sense to use its position (0.06 Å above the C1C3C5 plane in the case of **1a**) to define the geometrical HA parameter  $P$  (vide infra). Parameter  $P$ , folding angle  $\zeta$ , calculated charges at C3, and orbital contributions to  $\sigma(\text{C}3)$  as well as  $\sigma(\text{C}3)$  itself all correlate with each other, thus confirming that they all reflect in some way the HA character of the cation in question. The folding angle determines the overlap  $S(w_s, p\pi)$  between the symmetric Walsh orbital of the cyclopropane unit and the  $p\pi(\text{C}3)$  orbital. The closer the resulting 2e3c orbital is located to C3 ( $P$  values close to 1), the stronger the through-space orbital interactions and the charge transfer from the three-membered ring to C3 are (which of course also depends on the orbital energy difference  $\epsilon(w_s) - \epsilon(p\pi)$ ). As a consequence, the  $p\pi$  orbital is partially filled, positive charge at C3 is diminished, local paramagnetic ring currents are strongly reduced, and  $\sigma(\text{C}3)$  is dominated by a diamagnetic (shielding) contribution of the 2e3c-LMO. We conclude that, experimentally, HA character of cations such as **1a** is best recognized by the  $^{13}\text{C}$  shift value of C3.

Proton chemical shifts also depend on the nature of the electronic interactions that are characteristic of trishomocyclopropenylium cations. For a variation of C1C5 from 1.5 to 2.4 Å,  $^1\text{H}$  shift values change by maximally 3 ppm. However,  $\delta^1\text{H}$  values normally depend on environmental effects much more than  $\delta^{13}\text{C}$  values and, therefore, are often not very useful for analysis of the electronic structure by theoretical means. Nevertheless, it is interesting to note that, at the equilibrium

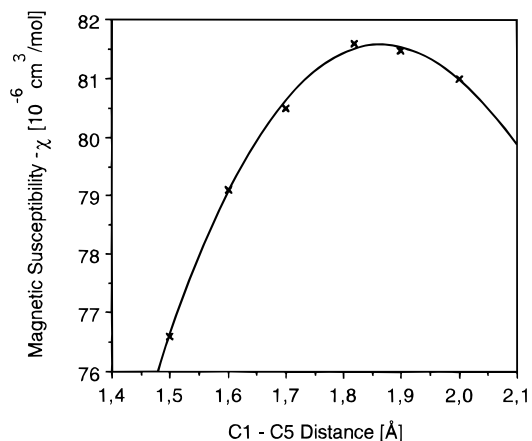


**Figure 11.** Calculated magnetic susceptibility  $\chi$  of cation **1** given as a function of distance C1C5 (IGLO/6-31G(d) calculations).

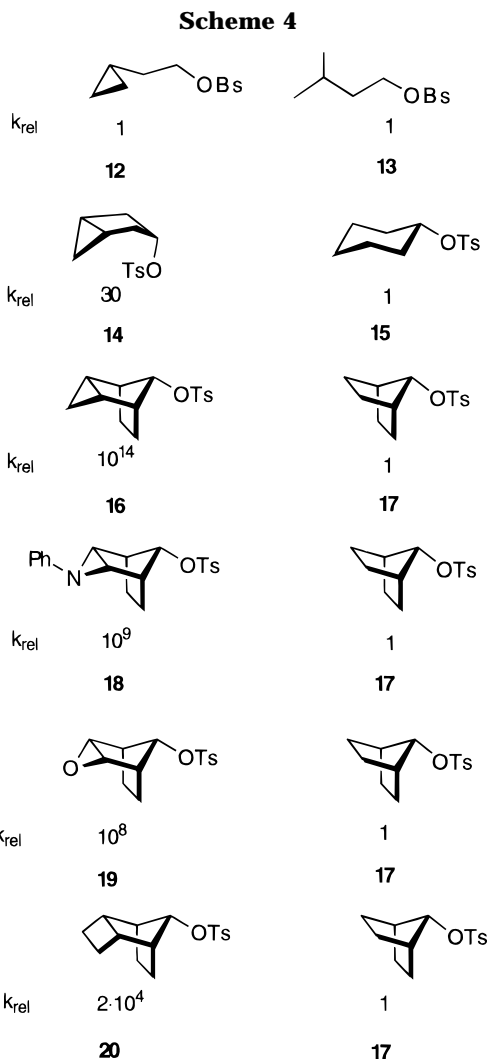
geometry of **1a**, IGLO and experimental  $^1\text{H}$  shifts agree within 0.3 ppm (Table 3).

The magnetic susceptibility  $\chi$  of **1a** also depends on changes in distance C1C5 (Figure 11). For C1C5 = 1.835 Å, a maximum is reached ( $-\chi = 81.4 \cdot 10^{-6} \text{ cm}^3 \text{ mol}^{-1}$ ) similar to the case of the monohomotropylum cation.<sup>9</sup> It seems that a maximal value of  $\chi$  is closely connected with HA electron delocalization and, therefore, can also be used as an indicator for the HA character of a trishomocyclopropenylum cation.

### 8. Chemical Relevance of *ab Initio* Investigations: Anchimeric Assistance in Solvolysis

In Scheme 4, measured rate acceleration data for the solvolysis of various bicyclo[3.1.0]hex-3-yl tosylates caused by anchimeric assistance of the cyclopropyl ring are summarized.<sup>61–65</sup> It is clear that for effective through-space interactions between the symmetric Walsh orbital of the three-membered ring and the developing  $p\pi(\text{C}3)$  orbital certain geometrical requirements have to be fulfilled. These are given by the carbon framework of a cis-substituted bicyclo[3.1.0]hexane derivative but not by an acyclic hydrocarbon that possesses cyclopropyl and leaving group in 1,3 positions. For example, no anchimeric assistance has been observed for the acetolysis of 2-cyclopropylethyl brosylate (**12**) as compared to that of isoamyl brosylate (**13**),<sup>61</sup> while the acetolysis of *cis*-bicyclo[3.1.0]hex-3-yl tosylate (**14**) is 30 times faster than that of cyclohexyl tosylate (**15**, Scheme 4).<sup>3,19,66</sup> The effect of the cyclopropyl group is relatively small because **14** first has to undergo ring inversion before anchimeric assistance in the solvolysis reaction is possible.

If the bicyclo[3.1.0]hex-3-yl unit of the substrate is already fixed in a conformation that satisfies the stereo-electronic requirements of HA, increased anchimeric acceleration can be observed. For example, in *endo*-tricyclo[3.2.1.0<sup>2,4</sup>]oct-*anti*-8-yl tosylate (**16**) the bicyclo[3.1.0]hexyl unit is forced by the C2C4-ethano bridge into



the chair conformation (folding angle  $\zeta$  is about  $120^\circ$ ) and, accordingly, anchimeric assistance increases the rate of solvolysis by a factor of  $10^{14}$  (Scheme 4) compared to the 7-norbornyl tosylate (**17**), which should have a similar folding angle.<sup>63</sup> Cation **16** has a  $\delta^{13}\text{C}8$  value of 0 ppm which suggests a folding angle of  $88^\circ$  (Figure 9) and somewhat stronger HA character than in the case of **1a**.

A methyl group at C3 can hinder the formation of cation **1a**. For example, Olah and co-workers<sup>22</sup> and Kelly and co-workers<sup>24</sup> report that 3-methyl-*cis*-bicyclo[3.1.0]hexan-3-ol does not form the HA cation **1a** in  $\text{SbF}_5/\text{SO}_2\text{-ClF}$  at  $-80^\circ\text{C}$  but rearranges to the 3-methylcyclohexenyl cation. On the other hand, *endo*-8-methyltricyclo[3.2.1.0<sup>2,4</sup>]octan-*anti*-8-ol (*endo*-8-methyl-**16**-8-ol) can be ionized to the *endo*-8-methyltricyclo[3.2.1.0<sup>2,4</sup>]oct-8-yl cation (*endo*-8-methyl-**16a**), for which a  $\delta^{13}\text{C}8$  value of 29.1 ppm has been measured.<sup>24</sup> These observations can be easily explained on the basis of *ab initio* results obtained in this work. A methyl group donates negative charge to the  $p\pi$  orbital of C8 via hyperconjugation, and thereby, the  $p\pi(\text{C}8)$  orbital is less available for through-space interactions. (Actually, the energy of the  $p\pi(\text{C}8)$  orbital is raised by interactions with the pseudo- $\pi$  orbital of the methyl group leading to an increase of the energy difference  $\epsilon(w_s) - \epsilon(p\pi)$  and a reduction of through-space interactions.) Methyl-substituted **1** is no longer stabilized by HA in the same way as the parent cation itself and, therefore, can form just the envelope form **1c** (if at

(61) Rhodes, Y. E.; Takino, T. *J. Am. Chem. Soc.* **1968**, *90*, 4469.

(62) Sakai, M.; Diaz, A.; Winstein, S. *J. Am. Chem. Soc.* **1970**, *92*, 4452.

(63) Gassman, P. G.; Schaffhausen, J. G.; Starkey, F. D.; Raynolds, P. W. *J. Am. Chem. Soc.* **1982**, *104*, 6411.

(64) Gassman, P. G.; Schaffhausen, J. G.; Raynolds, P. W. *J. Am. Chem. Soc.* **1982**, *104*, 6408.

(65) Hornback, J. M. *J. Org. Chem.* **1973**, *38*, 4122.

(66) Fainberg, A. H.; Winstein, S. *J. Am. Chem. Soc.* **1956**, *78*, 2780.

all), which then rearranges by various [1,2] H-shifts to more stable cations such as the 3-methylcyclohexenyl cation.<sup>22</sup>

For the *endo*-8-methyl-**16a** cation, the chair form is enforced, and therefore, a HA cation is formed. Methyl substitution of cyclopentyl cation leads to a 17 ppm downfield shift at the substituted C atom.<sup>67</sup> In the case of the *endo*-8-methyl-**16a** cation, a downfield shift of 29 ppm has been measured,<sup>24</sup> which suggests that the methyl effect is about double as large. Obviously, diamagnetic shielding effects resulting from HA 2e-delocalization are reduced and paramagnetic deshielding effects involving the C8C LMOs are increased. If one uses the relationship between C3 (C8) shift value and folding angle  $\zeta$  shown in Figure 9, then  $\zeta = 95^\circ$  will result. Hence, the *endo*-8-methyl-**16a** cation is less HA than the corresponding parent cation.

When the cyclopropane unit of **16** is replaced first by aziridine, then oxirane, and, finally, cyclobutane, thus leading to compounds **18**, **19**, and **20** in Scheme 4, the relative rate constant for hydrolysis is reduced stepwise by several powers of 10 (see Scheme 4), but in each case  $k_{\text{rel}}$  is considerably larger than the value for **17**. These observations are in line with the ab initio results obtained in this work. Heteroatoms such as N or O decrease the orbital energy of the symmetric Walsh orbital and, thereby, anchimeric assistance and HA character of the intermediate cation. For cyclobutane, this effect is largest but even then some residual HA character and anchimeric assistance remains. The HA stabilization energies given in Table 5 correlate roughly ( $r^2 = 0.92$ ) with  $\log k_{\text{rel}}$  of compounds **16** and **18–20** (Scheme 4). Actually, a better correlation cannot be expected since the ethano bridges will lead to considerable changes in the HA energies. Also, one has to consider that the HA stabilization energies given in this work cover in addition strain, inductive, and hyperconjugative effects that cannot be segregated (vide infra).

Without an ethano bridge, heteroatoms such as N or O may hinder the formation of an intermediate trishomocyclopropenylium cation. For the acetolysis of 6-oxa-bicyclo[3.1.0]hex-3-yl tosylate, anchimeric assistance has been excluded on the basis of kinetic measurements and the observed product distribution.<sup>65</sup> The oxirane ring is probably not able to provide sufficient anchimeric assistance for heterolytic bond cleavage. If a  $S_N1$  reaction takes place at all in the case of 6-oxa-**14**, through-space interactions are not strong enough to cause a stronger folding of the chair form. It is most likely that the intermediate cation (starting from about  $\zeta = 150^\circ$  in the parent compound, see **2c**, Table 1) is formed with a  $\zeta$  value larger than  $134^\circ$ , which defines the position of the TS for chair–envelope inversion in the case of cation **8**. Therefore, cation **8c** will be formed first, which then has the choice of either inverting back to the HA chair form (barrier 12.5 kcal/mol, Table 2) or rearranging to a 6-oxa-**5** cation (barrier smaller than 1 kcal/mol). Even if a  $S_N1$  mechanism applies to the solvolysis of 6-oxa-**14**, there is very little chance of HA intermediate **8a** forming.

Similar considerations apply to *cis*-bicyclo[3.2.0]hept-3-yl tosylate (**21**). Meinwald and co-workers<sup>68</sup> have

shown that in the acetolysis of **21** predominantly inverted acetate was obtained, which is incompatible with anchimeric assistance and indicates a  $S_N2$  mechanism for the reaction. It would be interesting to enforce a  $S_N1$  mechanism for the solvolysis of **21** and to test whether the ethano-bridged center-protonated spirocyclopentyl cation **10a** is formed. Of course, there is a high probability that the envelope form **9c** is formed followed by subsequent rearrangement to a bicyclo[3.2.0]hept-2-yl cation (**22**), which is known to further rearrange to the 7-norbornyl cation.<sup>69</sup> The energy barrier for the conversion of **9c** to **10a** is just 6 kcal/mol while the energy difference between these forms is 11.5 kcal/mol in favor of cation **10a**. Since the activation energy for a rearrangement to a 7-norbornyl cation is 16.1 kcal/mol, there will be a chance of generating and investigating cation **10a** if the formation of **22** can be avoided. We are presently investigating this possibility.

## 9. Conclusions

1. The trishomocyclopropenylium cation **1a** is clearly a nonclassical cation with HA 2e-delocalization in the cycle C1C3C5 as first predicted by S. Winstein.<sup>1,2,19,20</sup> This is indicated by the calculated molecular properties of **1a**.

(a) The through-space interaction distances C1C3 and C3C5 (1.82 Å), which are a result of a folding angle  $\zeta$  of  $87^\circ$ , are typical of HA molecules investigated so far.<sup>9–14</sup>

(b) The exact HA stabilization energy cannot be calculated because of strain and hyperconjugative effects in **1a**, but as a lower limit we estimate for it a value of 17 kcal/mol given by the classical cation **1c**.

(c) Because of HA, the positive charge of **1a** is delocalized in the cycle C1C3C5. In addition, the CH<sub>2</sub> groups carry some of the positive charge as a result of hyperconjugation.

(d) The HA character of **1a** is best reflected by the  $\delta^{13}\text{C}$  values of C1, C3, and C5 (0.9 ppm), which are 350 ppm shifted to higher field compared to those of a classical carbocation.

(e) The magnetic susceptibility  $\chi$  ( $-81.5 \times 10^{-6} \text{ cm}^3 \text{ mol}^{-1}$ ) of **1a** adopts a maximum value at the equilibrium geometry.

2. HA in **1a** is the result of through-space interactions between the symmetric Walsh orbital of the cyclopropane ring and the  $p\pi$  orbital at C3. These orbital interactions lead to charge transfer from C1C5 to C3 and to the formation of a two-electron, three-center (2e3c) orbital that seems to be typical of all trishomocyclopropenylium cations.

3. The degree of trishomocyclopropenylium character in **1a** is reflected by the magnitude of the distance C1C5, the folding angle  $\zeta$ , the position  $P$  of the 2e3c-orbital, the charge at C3, the  $^{13}\text{C}$  or  $^1\text{H}$  shift value of C3H, and the 2e3c-, C2C3-, or C3H-LMO contributions to  $\sigma(^{13}\text{C}3)$ , which all correlate with each other (Figures 7–10). For example, experimental  $\delta^{13}\text{C}$  values can be used to determine the folding angle  $\zeta$  of a trishomocyclopropenylium cation.

4. Perturbation of **1a** by a change of the distance C1C5 ( $C_s$  symmetry constraint) leads to a slow decrease of tris-HA (C1C5 stretching force constant 1.05 mdyn/Å). For C1C5 = 1.50 Å and a fully developed cyclopropane ring (form **1d**), there is still HA character in **1d** (cyclopropyl HA) as indicated by calculated charges, shift values

(67) Myhre, P. C.; Kruger, J. D.; Hammond, B. L.; Lok, S. M.; Yannoni, C. S.; Macho, V.; Limbach, H. H.; Vieth, H. M. *J. Am. Chem. Soc.* **1984**, *106*, 6079. Botkin, J. H.; Forsyth, D. A.; Sardella, D. J. *J. Am. Chem. Soc.* **1986**, *108*, 2777.

(68) Meinwald, J.; Anderson, P.; Tufariello, J. J. *J. Am. Chem. Soc.* **1966**, *88*, 1301.

(69) Winstein, S.; Gadiant, F.; Stafford, E. T.; Klinedinst, P. E. *J. Am. Chem. Soc.* **1958**, *80*, 5896.

( $\delta^{13}\text{C3} = 109$  ppm), and a relative energy of 12 kcal/mol compared to that of **1a**. Perturbation of **1a** under  $C_{3v}$  symmetry constraint leads to a steeper increase of the PES (breathing force constant: 3.5 mdyne/Å). In summary, HA is more pronounced in **1a** than in the monohomotropylium cation.

5. Bicyclo[3.1.0]hexane (**2**), which is the neutral parent compound of cation **1a**, is most stable in the boat form **2c**. There exists a chair form **2a**, which is 3.6 kcal/mol higher in energy. However, form **2a** is located in a flat local minimum that after ZPE and temperature corrections becomes just a shoulder of the ring-puckering potential of **2** (Figure 4). This explains previous contradictions between theoretical and experimental descriptions of possible conformations of **2**.<sup>28,30,49–51</sup>

6. Because of conclusion 5, it is likely that the formation of **1a** in solvolysis reactions of cis derivatives of **2** requires excitation of large amplitude puckering vibrations of the boat form to give the chair form before heterolytic C3–X bond cleavage can occur. For cis derivatives of **2** with a more pronounced chair minimum, boat–chair inversion precedes the bond cleavage process.

7. Cation **1a** can invert (barrier 26 kcal/mol) at increased temperatures to an envelope conformation **1c** that is 17 kcal/mol less stable than **1a**. Form **1c** has all properties of a classical carbocation and, therefore, can be used as a reference for **1a**.

8. The envelope form **1c** easily rearranges (barrier: 1 kcal/mol) to the bicyclo[3.1.0]hex-2-yl cation (**5a**) by a shift of the trans H atom at C2. Cation **5a** is 3 kcal/mol more stable than **1a** because it contains a cyclopropyl-carbinyl cation unit.

9. Remote perturbation of HA interactions by a heteroatom at position 6 change the energy and amplitude of the symmetric Walsh orbital and, thereby, HA interactions. Boron as an electropositive element increases HA interactions (relative stabilization energy  $\Delta E = -2.4$  kcal/mol) while nitrogen and oxygen decrease HA interactions in the trishomocyclopropenylium cation ( $\Delta E = 4.6$  and 15.2 kcal/mol). This trend is also reflected by the fact that with increasing electronegativity of the heteroatom (BH, CH<sub>2</sub>, NH, O) the chair–envelope energy

difference (21.7, 16.8, 8.2, 2.7 kcal/mol) and the chair–envelope inversion barrier (29.3, 25.4, 19.4, 10.8 kcal/mol) become smaller. Ab initio calculations explain why for *cis*-6-oxabicyclo[3.1.0]hex-3-yl tosylate anchimeric assistance was not observed.<sup>65</sup>

10. Replacement of the cyclopropane ring of **1a** by a cyclobutane ring leads to strong reduction of HA interactions. The nonclassical cation **9a** no longer exists; a minimum is only found for the classical cation **9c**. Anchimeric assistance by the cyclobutane ring is not possible.<sup>67</sup>

11. Cation **9** can rearrange to the norbornyl cation via the ethano-bridged center-protonated spirocyclopentyl cation **10a**, which can be formed by opening of the bond C1C5 of the envelope form **9c** (barrier 9 kcal/mol). Cation **10a** rearranges to the 7-norbornyl cation via an energy barrier of 16 kcal/mol. Since **10a** contains a pentacoordinated C atom, its structure and electronic properties make **10a** an interesting target for synthesis.

12. If the bicyclo[3.1.0]hex-3-yl unit of a potentially tris-HA molecule is “prefolded” by the existence of a C2C4-ethano bridge, the stereoelectronic requirements for HA interactions are enforced even in those cases in which an electronegative heteroatom or a cyclobutane ring should decrease HA. Considering this point, kinetic acceleration data summarized in Scheme 4 can all be explained with the ab initio results obtained in this work.

**Acknowledgment.** This work was supported by the Swedish Natural Science Research Council (NFR). K. J. Szabo thanks the NFR for a postdoctoral stipend. All calculations were done on the CRAY YMP of the Nationellt Superdatorcentrum (NSC), Linköping, Sweden. The authors thank the NSC for a generous allotment of computer time.

**Supporting Information Available:** Cartesian coordinates of HF and MP2 optimized geometries for **1–10** (23 pages). This material is contained in libraries on microfiche, immediately follows this article in the microfilm version of the journal, and can be ordered from the ACS; see any current masthead page for ordering information.

JO951927Y